

G-CSF Control of Neutrophils Dynamics in the Blood

E. Shochat*, V. Rom-Kedar, L.A. Segel

Weizmann Institute of Science, Rehovot, Israel

Received: 26 July 2006 / Accepted: 16 March 2007 / Published online: 7 June 2007
© Society for Mathematical Biology 2007

Abstract White blood cell neutrophil is a key component in the fast initial immune response against bacterial and fungal infections. Granulocyte colony stimulating factor (G-CSF) which is naturally produced in the body, is known to control the neutrophils production in the bone marrow and the neutrophils delivery into the blood. In oncological practice, G-CSF injections are widely used to treat neutropenia (dangerously low levels of neutrophils in the blood) and to prevent the infectious complications that often follow chemotherapy. However, the accurate dynamics of G-CSF neutrophil interaction has not been fully determined and no general scheme exists for an optimal G-CSF application in neutropenia. Here we develop a two-dimensional ordinary differential equation model for the G-CSF—neutrophil dynamics in the blood. The model is built axiomatically by first formally defining from the biology the expected properties of the model, and then deducing the dynamic behavior of the resulting system. The resulting model is structurally stable, and its dynamical features are independent of the precise form of the various rate functions. Choosing a specific form for these functions, three complementary parameter estimation procedures for one clinical (training) data set are utilized. The fully parameterized model (6 parameters) provides adequate predictions for several additional clinical data sets on time scales of several days. We briefly discuss the utility of this relatively simple and robust model in several clinical conditions.

Keywords G-CSF · Neutrophils · Mathematical dynamics · PK/PD

1. Introduction

The neutrophils are a principal part of the white blood cells system which defends the organism against acute bacterial and fungal infections (Kenneth et al., 2000). Normally the number of neutrophils in the blood is stationary. Following the onset of infection, their

*Corresponding author.

E-mail addresses: eliezer.shochat@weizmann.ac.il (E. Shochat), vered.rom-kedar@weizmann.ac.il (V. Rom-Kedar).

Dedicated to Lee Segel who guided us to apply mathematics for the benefit of mankind—a teacher, a colleague, a friend.

L.A. Segel passed away on 31 January 2005.

blood level surges dramatically within hours and stays high until the infection resides. On the other hand, anticancer chemotherapy causes the neutrophil density in the blood to plummet within a few days. Typically their level recovers to the pretreatment values in approximately a week or two. When the neutrophil density drops below a threshold level¹ major complications may arise due to the consequent suppression of the primary immune response which may lead to fulminate infections (Bodensteiner and Doolittle, 1993). Indeed, the risk of infection following chemotherapy is strongly correlated with the extent and the duration of neutropenia (Crawford et al., 2004). Furthermore, the occurrence of neutropenia and the complications associated with it, often lead to a delay in the optimal schedule of the chemotherapy administration that decreases the chances for a successful treatment (Donnelly et al., 2000). It is generally held by clinicians that the final steps in the neutrophil production and arrival to the blood are controlled by the granulocyte colony stimulating factor (G-CSF), a single peptide that is naturally secreted by numerous cells in response to an infection (Bronchud et al., 1988). G-CSF injections are widely used to prevent and treat neutropenia and the infectious complications that follow. However, despite the extensive use of G-CSF in the clinic, there are several issues regarding the treatment with G-CSF which are debatable. The most important of these is the observation that in some cases the G-CSF injections do not succeed to prevent the neutropenia whereas in others they do, with no clear understanding nor predictive tools to distinguish between these cases (Clark et al., 2005). The optimal scheduling and the a priori decision whether G-CSF is needed for a particular patient are other important issues that are not fully determined (Bennett et al., 1999). A natural question arises whether an efficient mathematical model, that is applicable to the management of chemotherapy induced neutropenia in individual oncological patients under relevant clinical conditions, can be constructed.

It is postulated that the cancer chemotherapy temporary interference with neutrophil production in the bone marrow is the main mechanism for the chemotherapy induced neutropenia. Neutrophils originate from pluripotent stem cells that reside in the bone marrow via a multi-step process that is shown to be controlled by several stimulatory and inhibitory hematopoietic growth factors (Moore, 1991; Ratajczak and Gewirtz, 1995). Indeed, a complete description of the neutrophils production process inherently involves a large network of cell lines and growth factors and it may depend non-trivially on the concentration of the bacteria in the tissue, on various metabolic substances and on their spatial distributions. Notably, the quantitative and qualitative biological information regarding the various paths in this large system is still incomplete.

The impact of granulopoiesis modeling was recently reviewed by Friberg and Karlsson (2003). Indeed, numerous mathematical models of the neutrophil production—also termed granulopoiesis—have been suggested over the years (Rubinow and Lebowitz, 1975; Lajtha et al., 1962; King-Smith and Morley, 1970; Blumenson and Bross, 1979; Abkowitz et al., 1996; Bernard et al., 2003; Zamboni et al., 2001; Krzyzanski et al., 1999; Shochat and Stemmer, 2002; Ostby et al., 2003; Scholz et al., 2005; Vainstein et al., 2005; Panetta et al., 2003; Wang et al., 2001; Foley et al., 2006; Haurie et al., 2000). Each of the models showed a good agreement with *some* empirical data. A number of these models were specifically developed to mathematically capture *the detailed biology* of the bone marrow (Rubinow and Lebowitz, 1975; Blumenson and Bross, 1979;

¹Severe neutropenia is defined as one order decrease in the neutrophil count (from normal levels of $\approx 5000 \times 10^3$ cells/cc, to the dangerous levels of below 500×10^3 cells/cc).

Abkowitz et al., 1996; Shochat and Stemmer, 2002; Vainstein et al., 2005). Such models are intrinsically high dimensional, nonlinear and often contain large parameter sets. With these high dimensional models, the ability to estimate the parameters, study the dynamics and investigate the sensitivity of the solutions to changes in the initial conditions and parameters is limited. In particular, the large number of parameters (for example, a staggering 40 parameters in Shochat and Stemmer, 2002) practically precludes precise estimation and validation of the model. In clinical situations, we are typically able to observe only the blood counts corresponding to the final component of granulopoiesis while the underlying biology of the bone marrow that leads to the dynamics in the blood remains hidden from our view. Thus, only a minority of the parameters of a detailed model and only their relative order of magnitude can be accessed.

Several authors focused on more attainable restricted aspects of the granulopoiesis dynamics. In (Rubinow and Lebowitz, 1975; Ostby et al., 2003) the flux of neutrophils into the blood was modeled by partial differential equations (PDE's) that describe the evolution of the age structure in sub-populations of cells of the bone marrow. Such approach enabled to successfully track the long term evolution of neutrophils recovery following high dose chemotherapy and bone-marrow transplant (Ostby et al., 2003). In (Bernard et al., 2003; Foley et al., 2006; Haurie et al., 2000) the dependence of the neutrophils flux on the bone marrow history was modeled by using delayed differential equations (DDE's). In this framework, the G-CSF effects were implicitly represented by a negative feedback loop. This approach adequately describes the periodic behavior of the neutrophils levels in the clinical syndrome of cyclic neutropenia.

The analysis of both the PDEs and the DDEs equations is challenging. Behind the apparent simplicity of the succinct formulations lurks their inherently infinite dimensional nature. The dependence on the boundary conditions and the initial profile in the PDE case, or on the history profile in the DDE case is highly non-trivial.²

Finally, several low-dimensional ordinary differential equations models of granulopoiesis had been proposed. Zamboni et al. (2001) used a pharmacokinetic–pharmacodynamic approach to study the effect of blood concentrations of the chemotherapeutic drug Topotecan on neutrophil dynamics. Panetta et al. (2003) studied the dynamics of neutrophils following treatment with a chemotherapeutic drug Temozolomide and used the notion of negative feedback to successfully describe the control of the neutrophil levels following chemotherapy. However, these studies did not include the explicit dynamics of G-CSF. A detailed empirical study of the G-CSF effects was conducted by Wang et al. (2001), where a pharmacokinetic–pharmacodynamic model of the G-CSF blood concentrations effect on the neutrophil dynamics in the blood was introduced. In this study, the authors focused on the effect of a single G-CSF injection on healthy volunteers. Subsequently, neither the effects of chemotherapy nor the internal G-CSF production, which is dominant in the natural processes of recovery from chemotherapy induced neutropenia (Sallerfors, 1994), were addressed.

There is a two fold challenge to mathematical modeling of neutrophil dynamics as pertinent to oncological clinics. The first one is to equip the practicing clinician with

²It involves dependence on classes of functions, effectively corresponding to infinite number of parameters.

a relatively simple and robust mathematical model that will be useful in the everyday work. When approaching this task one uses the clinical principles and knowledge to construct the model. This first standard stage, of formulating the clinical principles by a mathematical framework, leads many times to important insight regarding the underlying biology. Yet, the inherent complexity of the problem at hand means that there may be inconsistencies in the underlying biological hypotheses of clinicians about the neutrophil dynamics. Thus, a second, more subtle challenge, is to examine by mathematical reasoning these possible *inconsistencies*. Here we use an axiomatic approach to construct the model (see details below). This allows us to refute a set of inconsistent biological assumptions. Furthermore, it enhances our confidence in the reliability of the consistent models, as these were constructed in a systematic formal way.

Despite, or perhaps in the wake of the apparent complexity of the system, it is generally held by clinicians that the neutrophil dynamics in the blood can, to large extent, be dominated by G-CSF (Bronchud et al., 1988). This viewpoint is supported by several distinct clinical observations as described in Section 2. Indeed, G-CSF injections are extensively used to handle neutropenia in cancer patients. Here we construct a model that specifically studies whether the neutrophil dynamics can be effectively represented by considering only the interactions of the G-CSF (G) and the neutrophils (N) concentrations in the blood. The model is defined by a system of two ordinary differential equations depending on a vector of parameters μ (see Fig. 3). To keep a tight grip on the biological assumptions that enter the model we adopt an axiomatic construction of the ODE's system. Thus, to construct the right-hand side of these equations, statements of the form “*an increase in G causes an increase in the production rate of N* ”, are translated to monotonicity conditions on the rate functions. The consistency and sufficiency of the clinical convention (we interpret such a convention as an underlying biological hypothesis), that neutrophils dynamics is mainly governed by the G-CSF and the neutrophil levels in the blood (see Fig. 3), is thus studied.

The manuscript is ordered as follows; in Section 2, based upon the biological properties, we axiomatically construct the general model of the G-CSF and neutrophils GN dynamics and prove that the resulting GN system has only one stable equilibrium point. In Section 3, we construct a specific model which satisfies the biological assumptions and study its properties. This model has five non-dimensional parameters which are estimated in Section 4 by two independent methods. Then the sensitivity of the equilibrium and the transients to parameter changes is investigated analytically. The section ends with a model validation. We use one detailed clinical data set (reported in Wang et al., 2001) as a training set to fit the parameters. We then demonstrate that the model with the obtained fixed parameters *predicts* additional clinical observations from Wang et al. (2001); a data set in which the same patient received double dose of G-CSF and data sets of another patient receiving two dose regimens are well described by the model without any fitting. The conclusions section includes reflections on our methodology, a list of clinical situations in which our model may be relevant, some predictions of the model, and a discussion of the conditions under which the two-dimensional model does not hold and its extensions must be considered.

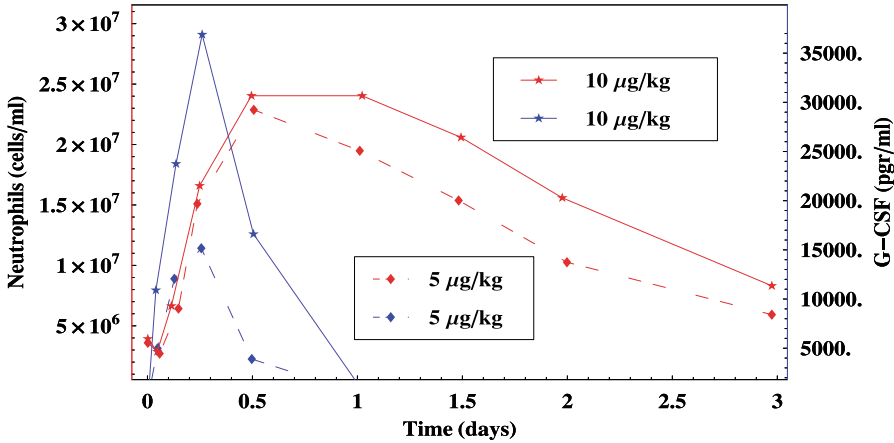


Fig. 1 G-CSF (blue) and neutrophil (red) dynamics in healthy volunteers following a single subcutaneous injection with either 5 µg/kg (dashed line) or 10 µg/kg of G-CSF (solid line) (data adapted from Van der Auwera et al., 2001). (Colour figure online.)

2. The axiomatic approach to GN dynamics

We postulate that the averaged concentrations of the G-CSF (G) and neutrophils (N) in the blood may be modeled by a system of two ordinary differential equations depending on a vector of parameters μ :

$$\begin{cases} \frac{dG}{dt} = f_1(G, N; \mu), \\ \frac{dN}{dt} = f_2(G, N; \mu). \end{cases} \quad (1)$$

The G-CSF and the neutrophil blood levels are nearly constant in a healthy person³ (Table 1) (Fliedner et al., 2002; Shochat and Stemmer, 2002), and only extreme perturbations in the system might prevent their complete natural restoration (Krishan et al., 1976; Fliedner et al., 2002). Their dynamics are coupled during perturbations: in humans that received G-CSF injections, neutrophil levels follow the increase of G-CSF in serum (Fig. 1). In chemotherapy induced neutropenia, the initial decrease in the neutrophils is promptly followed by an increase of intrinsic G-CSF secretion and a consequent recovery of the neutrophils (Bonig et al., 1999) (Fig. 2).

³Some evidence suggests that haematopoiesis exhibits subtle bi-harmonic behavior with short (24 hours) relatively low amplitude diurnal oscillations (Smaaland et al., 1992) superimposed on long (21 days) oscillations (Carulli et al., 2000). Although such oscillations do not appear in our simple model they may be introduced by including explicit circadian periodicity or a delay (Bernard et al., 2003) in the neutrophil production term, see conclusions section.

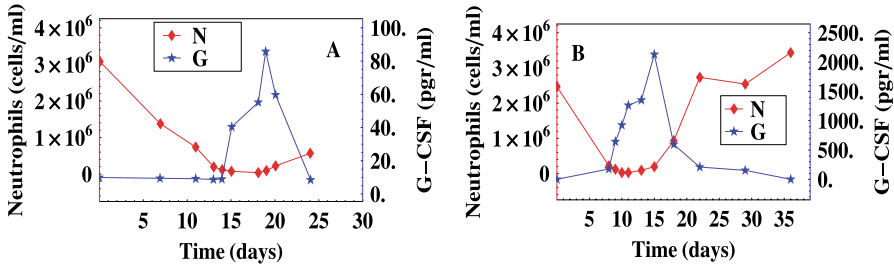


Fig. 2 Natural G-CSF and neutrophil dynamics in patients following anticancer chemotherapy. Blood neutrophils (N) and G-CSF (G) levels are labeled red and blue, respectively. Note the threshold neutrophil level of 500×10^3 cells/ml which triggers prompt increase in G-CSF levels. (A) Conventional chemotherapy in lung cancer patients (data adapted from Takatani et al., 1996). (B) High dose chemotherapy in children with hematological malignancies (data adapted from Saito et al., 1999). Note the different scales of the G-CSF levels on the two panels. (Colour figure online.)

To formulate explicitly the known properties of the growth rate functions $f_{1,2}$, it is helpful to consider the “birth” processes $B(X; \mu)$ and “death” processes $D(X; \mu)$ separately,⁴ with $X = (G, N) \in R_+^1 \times R_+^1$:

$$f_i(X; \mu) = B_i(X; \mu) - D_i(X; \mu), \quad i = 1, 2, \tag{2}$$

where the terms B_i and D_i denote the respective non-negative, smooth and bounded birth and death rate functions of each variable:

$$\forall X, \mu; \quad \begin{cases} 0 \leq B_i \leq B_i^{\max}, \\ 0 \leq D_i \leq D_i^{\max}. \end{cases} \tag{3}$$

Our variables represent densities of real physical entities ($G = \frac{\text{pgrams}}{\text{ml}}$ and $N = \frac{\text{cells}}{\text{ml}}$) so the variables must be non-negative and bounded by some maximal values.⁵ Thus, the domain $\mathcal{D} = \{(G, N) \in [0, G^{\max}] \times [0, N^{\max}]\}$ must be invariant under the forward dynamics:

$$B_i(\mathbf{X}; \mu) - D_i(\mathbf{X}; \mu)|_{X_i=0} \geq 0, \tag{4}$$

and

$$B_i(\mathbf{X}; \mu) - D_i(\mathbf{X}; \mu)|_{X_i=X_i^{\max}} \leq 0. \tag{5}$$

⁴“Birth” includes hereafter all forms of production of the i th entity, including incoming migration and reproduction. Similarly, “death” includes all forms of elimination including migration, consumption and senescence.

⁵The maximal physical values of cell density N^{\max} are given by $\frac{\text{unit volume}}{\text{volume/cell}}$ and are of the order of 10^9 cells. This should not be identified with the carrying capacity of the cell population in the blood, which is lower due to viscosity and metabolic constraints and is of the order of 10^8 cells/cc (Zarkovic and Kwaan, 2003), nor with the typical density of neutrophils which is much smaller, see Table 1. The maximal physical values of blood G-CSF reflect the precipitation property of the molecule, and are in the order of 80 mg/cc (Krishnan et al., 2002), again a much higher value than the typical concentrations used in the clinic.

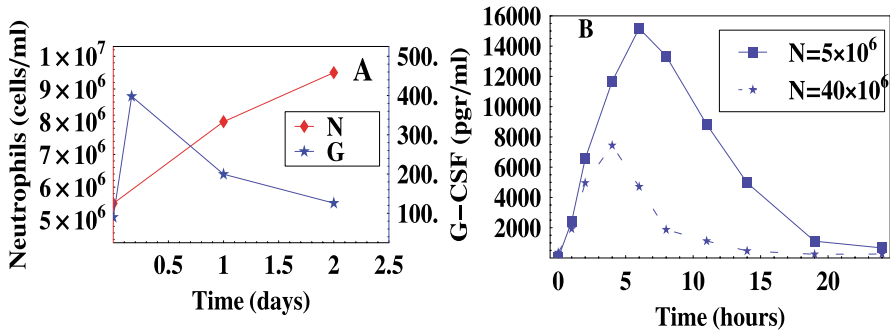


Fig. 4 (A) A typical example of GN dynamics following potentially infective insult of thoracic surgery (data adapted from Noursadeghi et al., 2005). Blood neutrophils (N) and G-CSF (G) levels are labeled red and blue, respectively. (B) G-CSF kinetics in volunteers on day 1 (dashed blue line) and day 4 (solid blue line) of sequential G-CSF injections (data adapted from Kroger et al., 2004). Note the high G-CSF levels at day 1 (baseline neutrophil count of $\approx 5 \times 10^6$ cells/ml. G-CSF lower levels on day 4 correspond to significantly higher blood neutrophil count ($\approx 40 \times 10^6$ cells/ml). (Colour figure online.)

production of G , and the relation here is not strictly *causal*.⁸ To adequately model the dynamics, it is sufficient to observe that an increase in N is *correlated* with a decrease in the production of G .

- (D_G) The elimination of G-CSF in the blood is relatively fast (Saito et al., 1999; Pigoli et al., 1982). G-CSF has a major first order (linear with G) elimination by the kidneys (Stute et al., 1992). In addition, G-CSF is directly consumed by the hematopoietic cells and the blood neutrophils (Terashi et al., 1999; Sarkar and Lauffenburger, 2003) (Fig. 4B). It follows that the total G-CSF clearance may be written in the form $D_G = D_G^r \cdot G + D_G^N(G, N)$, where D_G^r is a constant and D_G^N is a non-decreasing bounded function of G and N , satisfying $D_G^N(0, N) = D_G^N(G, 0) = 0$.
- (B_N) Blood neutrophils are created at the bone marrow where the cell renewal and differentiation are tuned by an array of signals (Ladd et al., 1997). The neutrophil flux into the blood is regulated by G-CSF (Bronchud et al., 1988). This factor binds to high affinity membrane receptors on marrow cells causing stimulation, expansion and maturation of the neutrophil pool and an increase in the transition of neutrophils to the blood (Sachs, 1992; Lord et al., 1989). Thus, $B_N = B_N(G)$ is an increasing function of G . Neutrophils are produced even without G-CSF effect (Bonilla et al., 1989; Lieschke et al., 1994) so that $B_N(0) > 0$.
- (D_N) Once in circulation, the blood neutrophils may migrate to the extra-vascular space or undergo senescence (elimination via aging) (Cronkite, 1979), so $D_N = D_N^{\text{mig}}(G, N) + D_N^{\text{sen}}(G, N)$. Colotta et al. (1992) reported an in-vitro study showing that the major effect of G-CSF on the blood neutrophils is to attenuate the intravascular senescence of these cells and prolong their survival by delaying apoptosis,⁹ hence: $D_N^{\text{sen}} = D_N^{\text{sen}}(G) \cdot N$ where $D_N^{\text{sen}}(G)$ is a decreasing function of G

⁸See Freedman (2004) for a recent formal discussion of causality and modeling.

⁹The estimated half-life of the in-vitro cells was 35 hours for untreated and 115 hours for G-CSF treated cells.

(Colotta et al., 1992; Mukae et al., 2000). On the other hand, it was suggested by de Haas et al. (1994) that immediately after a G-CSF injection the most activated neutrophils are induced to leave circulation to the extra-vascular space, so $D_N^{mig}(G, N)$ is an increasing function of G . The two opposing G-CSF effects on the circulating neutrophils seem to balance each other: two extensive clinical studies did not reveal a significant G-CSF effect on either neutrophil margination into the extravascular space or the cell's half life (Price et al., 1996; Lord et al., 1989). Hence, while the details of these balancing effects deserve a separate study, we take here a constant elimination rate of the neutrophils¹⁰: $D_N(G, N) = D_N \cdot N$.

2.2. General model formulation

The above observations lead to equations of the following form:

$$\begin{aligned} dG/dt &= B_G(N) - [D_G^r \cdot G + D_G^N(G, N)], \\ dN/dt &= B_N(G) - D_N \cdot N, \end{aligned} \tag{6}$$

where all the above coefficients and functions are non-negative and smooth, the variables are in \mathcal{D} and all the functions are monotone:

$$\begin{aligned} \frac{\partial B_G(N)}{\partial N} &\leq 0, & \frac{\partial D_G^N(G, N)}{\partial G} &\geq 0, \\ \frac{\partial B_N(G)}{\partial G} &> 0, & \frac{\partial D_G^N(G, N)}{\partial N} &\geq 0. \end{aligned} \tag{7}$$

From these properties, we establish that:

$$\begin{aligned} B_G(N^{\max}) &> 0, & D_G^N(0, N) &= 0, & D_G^N(G, 0) &= 0, \\ B_N(0) &> 0, & D_N &> 0. \end{aligned} \tag{8}$$

The following conditions guarantee that the domain \mathcal{D} remains invariant:

$$\begin{aligned} \forall N \geq 0; & \quad B_G(N) < D_G^r \cdot G^{\max} + D_G^N(G^{\max}, N), \\ \forall G \geq 0; & \quad B_N(G) < D_N \cdot N^{\max}. \end{aligned} \tag{9}$$

2.3. Stability properties of the general model

To obtain quantitative, practical results, we introduce in the next section a specific functional form for the system (6) which satisfies all our axiomatic constraints. Yet, before turning to this practical part, we will show that the monotonicity of the birth and death functions are sufficient to guarantee, *independently of the specific form of these functions*,

¹⁰Theorem 2.1 is valid for the more general case $D_N = D_N(G) \cdot N$ where $D_N(G)$ is a non-increasing function of G : $\frac{\partial D_N}{\partial G} \leq 0$. Conditions under which $D_N(G)$ is non-monotone in G could be studied separately.

that the system (6) always has a simple asymptotic behavior: it has a fixed point in the positive quadrant¹¹ which is unique and stable and no other recurrent behaviors are possible. Furthermore, the structure of the null clines is monotone in the most general case.

Theorem 2.1. *Consider the system (6) satisfying the constraints (7–9). Then the system has a **unique stable fixed point** in the positive quadrant of the phase-plane, and there are no other closed orbits there.*

Proof: Consider the null-clines:

$$N_1(G) = \{(G, N) \in R^2 : f_1 = B_G(N) - [D_G^r \cdot G + D_G^N(G, N)] = 0\},$$

$$N_2(G) = \{(G, N) \in R^2 : f_2 = B_N(G) - D_N \cdot N = 0\}.$$

Since $\frac{\partial f_{1,2}}{\partial N} \neq 0$ for all $(G, N) \in \text{int } \mathcal{D}$ (see (7), (8) and (10)), by the implicit function theorem these curves may be expressed as $\text{nc}_G = \{(G, N_1(G))\}$ and $\text{nc}_N = \{(G, N_2(G))\}$. Furthermore, the monotonicity property of the birth and death rates (7) implies that for $G > 0$, $N_1(G)$ is monotonically decreasing whereas $N_2(G)$ is monotonically increasing:

$$\frac{dN_1(G)}{dG} = \frac{D_G^r + \frac{\partial D_G^N(G, N)}{\partial G}}{\frac{\partial B_G(N)}{\partial N} - \frac{\partial D_G^N(G, N)}{\partial N}} < 0; \quad \frac{dN_2(G)}{dG} = \frac{\frac{\partial B_N(G)}{\partial G}}{D_N} \geq 0. \tag{10}$$

Hence, for positive G the curves $N_{1,2}(G)$ may have at most one intersection point—the fixed point (G^*, N^*) . Furthermore, it follows from (8) and (9) that $\frac{dG}{dt}|_{G=0} > 0$ hence, from (10) we conclude that $N_1(G) \rightarrow \infty$ as $G \rightarrow 0$. Since $N_2(0) = B_N(0)/D_N > 0$ is finite, there exists a small G for which $N_1(G) > N_2(G)$. On the other hand, these inequalities also imply that at $G = G^{\max}$, $\frac{dG}{dt} < 0$ for all $N \geq 0$, hence, $N_1(G^{\max}) < 0$ whereas $N_2(G^{\max}) = B_N(G^{\max})/D_N > 0$, namely $N_1(G^{\max}) < N_2(G^{\max})$. Thus, the two curves must intersect, and since $N_2(G) > 0$ for all $G \in [0, G^{\max}]$, their intersection occurs in the positive quadrant.

The stability of the fixed point is determined by the trace and determinant of the corresponding linearized matrix $J = J(G^*, N^*)$:

$$J(G, N) = \begin{bmatrix} -[D_G^r + \frac{\partial}{\partial G} D_G^N(G, N)] & B'_G(N) - \frac{\partial}{\partial N} D_G^N(G, N) \\ B'_N(G) & -D_N \end{bmatrix}.$$

Using (7), the sign of the trace and determinant of J is known for all $(G, N) \in \bar{\mathcal{D}}$:

$$\text{trace } J(G, N) = -\left[D_G^r + \frac{\partial}{\partial G} D_G^N(G, N) + D_N \right] < 0,$$

$$\det J(G, N) = \left[D_G^r + \frac{\partial}{\partial G} D_G^N(G, N) \right] D_N$$

$$- \left(B'_G(N) - \frac{\partial}{\partial N} D_G^N(G, N) \right) B'_N(G) > 0.$$

¹¹The origin is not a fixed point in this model since there is always a positive influx of neutrophils from the bone-marrow into the blood and of G-CSF from the tissue into the blood.

Since

$$\lambda_{1,2} = \frac{\text{trace } J}{2} \left(1 \pm \sqrt{1 - 4 \frac{\det J}{\text{trace}^2 J}} \right)$$

we establish that $\text{Re}\{\lambda_{1,2}\} < 0$ and thus the fixed point is stable. Furthermore, as $\text{trace } J(G, N) < 0$ for all $(G, N) \in \mathcal{D}$, by Bendixson's criterion (see Guckenheimer and Holmes, 2002 and references therein) and the strictly invariance¹² of \mathcal{D} there are no closed orbits which lie or partially lie in \mathcal{D} . The fixed point may be a node or a spiral depending on the relative size of $\det J$ and $\text{trace } J$:

$$\kappa = 4 \frac{\det J}{\text{trace}^2 J}; \quad \begin{cases} \kappa < 1 & \text{stable node,} \\ \kappa > 1 & \text{focus (stable spiral).} \end{cases} \quad (11)$$

□

Corollary 2.2. *The system (6) satisfying the constraints (7–9) is structurally stable.*

Proof: By Peixoto theorem (see Guckenheimer and Holmes, 2002 and references therein): \mathcal{D} is compact, simply connected two-dimensional region which is strictly invariant, the flow is smooth and it has a unique hyperbolic attracting fixed point (hence no heteroclinic connections). □

Notice that these results affirm that the axiomatic construction of our model is consistent with the observed robust dynamics; we did not require that a stable fixed point will appear nor that the system be structurally stable. These properties appeared as a result of the axiomatic construction, and these fit well the clinical observations that the neutrophils and G-CSF levels are nearly constant under physiological conditions (Fliedner et al., 2002; Shochat and Stemmer, 2002).

3. Specific model

Any set of functions which observes the constraints given by (7–9) will lead to the same dynamical behavior. This dynamic is asymptotically simple—it corresponds to exponential convergence to a stable fixed point. Indeed, the system (6) is a robust and structurally stable system—small changes in the functional form lead to small changes in the dynamics. Thus our model is well posed and a fitting procedure to the data should lead to a reasonable model. As our ultimate goal is to assist clinicians in the prediction and prevention of chemotherapy induced neutropenia for individual patients, we need to find the functional forms of the rate factors B_i, D_i for the system (6) that best fit the available clinical data. By choosing functional forms that are as simple as possible and depend on as small number of parameters as possible, we may be able to identify the dependence of the model predictions on the accompanying individual biological parameters. Finally, we note that the range of the clinically relevant initial conditions which is of interest is large, and cannot be modeled by the linearized dynamics alone. In particular, we will see

¹²It is easy to verify that the vector field points strictly inward on $\mathcal{D}'s$ boundary.

that the duration and extent of the transient behavior are crucial ingredients in the model fitting and in the predictive power of the theory.

For the present study, we have focused on variations of the familiar and venerable Michaelis–Menten (**MM**) formulation as the chosen specific functional forms of the birth and death terms. The **MM** formulations are often useful in pharmacodynamical calculations (Shochat and Stemmer, 2002). Notice that in the complex biological processes such as described here, unlike the simple enzyme dynamics, these forms have no immediate mechanistic meaning. When a large data set will be available one may attempt to refine and modify this choice.

3.1. Closed functional form

The form of $B_G(N)$: Fig. 2 demonstrates that the G-CSF blood level surges when the neutrophils level is decreased as expressed in (7). Thus, we postulate that N has a negative saturable effect on the G-CSF production rate, B_G :

$$B_G(N) = B_G^{\max} - \frac{B_G^{\max} \cdot N}{k_N + N} = \frac{B_G^{\max} \cdot k_N}{k_N + N}, \quad (12)$$

where k_N is a **MM** dissociation constant corresponding to the neutrophil density which induces a half-maximal production rate of G-CSF, and B_G^{\max} is the maximal rate of G influx to the blood.

The form of $D_G(G, N)$: The total G-CSF elimination is a superposition of two processes: the G-CSF renal clearance and the consumption of G-CSF by the blood neutrophils. Fukuda et al., conducted an extensive study of G-CSF clearance in lung cancer patients (Fukuda et al., 2001). Our analysis of this data suggests that G-CSF renal clearance is linear with G and proportional to the square of the creatinine clearance (a surrogate indicator of renal function). The neutrophil dependent G-CSF clearance is proportional to a **MM** function¹³ of N , which implies that the specific clearance per cell is decreasing as the cell density in the blood increases¹⁴ (see Section 4.1 and Fig. 7 for details). Thus,

$$D_G(G, N) = \left(D_G^r + \frac{D_G^n \cdot N}{k_N + N} \right) \cdot G, \quad (13)$$

where D_G^r is a function of the renal clearance (R_{CL}) and denotes the first order renal elimination parameter of G-CSF (Stute et al., 1992), while D_G^n denotes the neutrophil G-CSF elimination rate constant.

The form of $B_N(G)$: G-CSF regulates all stages of granulopoiesis, with a particular effect on late stage proliferation, neutrophil maturation and neutrophil influx to the blood.¹⁵

¹³It would have been natural to put a **MM** function of G as well, but the corresponding dissociation constant in this term would have been large, of $O(10^6)$ pcgrm/ml, so that for the physiological and medical ranges of G , of up to $O(10^4)$ pcgrm/ml, the dependence on G may be taken as linear. The asymptotic behavior of the model does not change if such a **MM** function is included.

¹⁴A possible explanation for the reduced specific G-CSF clearance is the high proportion of immature neutrophils with lower density of G-CSF receptors per cell that enter the blood from the bone marrow (Terashi et al., 1999).

¹⁵An estimated 3–5 extra divisions during neutrophil development and a shortening of maturation from 5 to only one day (Lord et al., 1989).

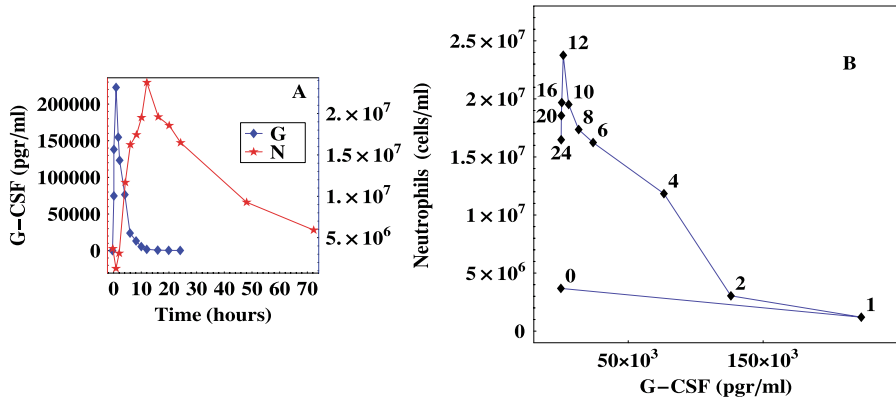


Fig. 5 G-CSF and neutrophil dynamics in healthy volunteers following single iv injection with 375 μg of G-CSF (data adapted from Wang et al., 2001). (A) Time course of blood neutrophils (N) (red) and G-CSF (G) (blue). (B) Phase portraits of the dynamics where numbers denote the time course of the trajectory. (Colour figure online.)

A typical GN dynamics following a single G-CSF injection is depicted in Fig. 5. To reflect the positive saturable effect of G-CSF on hematopoiesis we propose:

$$B_N(G) = B_N^{\min} + \frac{(B_N^{\max} - B_N^{\min}) \cdot G}{k_G + G}, \tag{14}$$

where B_N^{\min} denotes the background cell flux without “activator” G-CSF effect.¹⁶ The constant B_N^{\max} is the maximal activity and k_G is a corresponding **MM** dissociation constant (the G-CSF concentration which elicits half-maximal effect).

The form of $D_N(G, N)$: As discussed previously, we propose that the simple form:

$$D_N(G, N) = D_N \cdot N \tag{15}$$

is adequate to describe the overall balancing effects of G-CSF on neutrophil margination on one hand and on neutrophil intravascular senescence on the other (Price et al., 1996; Lord et al., 1989).

We arrived at the specific expression for the GN dynamics:

$$\begin{aligned} \frac{dG}{dt} &= \frac{B_G^{\max}}{1 + N/k_N} - \left(D_G^r + \frac{D_G^n \cdot N}{k_N + N} \right) \cdot G, \\ \frac{dN}{dt} &= \frac{B_N^{\min} k_G + B_N^{\max} \cdot G}{k_G + G} - D_N \cdot N. \end{aligned} \tag{16}$$

It can be shown that this system satisfies all the assumptions of the general model, and in particular, the domain \mathcal{D} is invariant for $G^{\max} > \frac{k_N B_G^{\max}}{D_G^r k_N}$ and $N^{\max} > \frac{B_N^{\max}}{D_N}$.

¹⁶See also Panetta et al. (2003) for a different version which does not include the effect of G-CSF explicitly.

To gain a better understanding of the nature of the dynamics, its time scales and the role of parameters, we introduce the following dimensionless variables:

$$\tau = t \cdot D_N, \quad g = \frac{100 \cdot G}{k_G}, \quad n = \frac{N}{10 \cdot k_N}, \tag{17}$$

where the numbers 100 and 10 are scaling factors that represent the ratios between the dissociation constants k_G and k_N and the corresponding typical G-CSF ($G^* \approx k_G/100$) and neutrophil ($N^* \approx 10k_N$) values. This choice of dimensionless variables ensures that (g, n) are of order one at the physiological steady state. Five dimensionless, positive parameters emerge:

$$\begin{aligned} a_1 &= 10 \frac{B_G^{\max}}{D_N k_G}, & a_2 &= \frac{D_G^r}{D_N}, & a_3 &= \frac{D_G^n}{D_N}, \\ a_4 &= \frac{1}{10} \frac{B_N^{\min}}{D_N k_N}, & a_5 &= \frac{B_N^{\max}}{B_N^{\min}}, \end{aligned} \tag{18}$$

and (16) becomes:

$$\begin{aligned} \frac{dg}{d\tau} &= \frac{a_1}{n + 0.1} - \left(a_2 + \frac{a_3 \cdot n}{n + 0.1} \right) \cdot g, \\ \frac{dn}{d\tau} &= a_4 \cdot \left(\frac{1 + 0.01 \cdot a_5 \cdot g}{1 + 0.01 \cdot g} \right) - n. \end{aligned} \tag{19}$$

In Section 4, we estimate the parameters and compare the behavior of this model with clinical data. Now we analyze the general behavior of the specific model for arbitrary values of the parameters.

3.2. Properties of the specific model

Although a closed-form analytical solution of the full non-linear system (19) is unknown, some important features may be found by studying the null-clines and the asymptotic form of the rate functions. In particular, we study *analytically* the fixed point dependence and sensitivity on the parameters, and then, we study *analytically* how the characteristic scales associated with the transient behavior depend on these parameters. The advantage of constructing a simple model is thus apparent.

First, by elementary algebra one can show that for all positive values of the parameters, the system (19) indeed has a unique stable fixed point in the positive quadrant (g^*, n^*) with $g^* \in (0, 10 \frac{a_1}{a_2})$. Provided the a_i are all of $O(1)$, the fixed point is given approximately by

$$g^* \approx \frac{a_1}{a_4(a_2 + a_3)}, \quad n^* \approx a_4 \tag{20}$$

and under these conditions the eigenvalues are approximately $\{-(a_2 + a_3), -1\}$ (see Appendix A.1 for derivation and conditions). Hence, under normal conditions, the neutrophil's asymptotic value (its fixed point value) is mainly¹⁷ controlled by a_4 . This para-

¹⁷As follows from the sensitivity analysis of the fixed point, see Section 4.5.

meter represents the background bone-marrow derived flux of neutrophils which is maintained when there is no infection (so g is of order one). This parameter is significantly reduced when the bone marrow is stunned by a chemotherapy treatment (see Section 4.4 and the conclusions).

Second, the transient behavior of the system¹⁸ when the neutrophils level is of order one and a sudden surge of G-CSF is introduced (e.g. by injection, so $n(0) = O(1)$, $g(0) \gg 1$) may be easily found (see Appendix A for details):

- (i) The extreme value of n at the transient stage (following the G-CSF injection) is mainly controlled by $a_4 \cdot a_5$.
- (ii) The transient time scale for the neutrophils dynamics is of order $\frac{1}{a_2+a_3} \ln g(0) + \ln(a_5 - 1)$.

This transient time scale may be further divided into three parts:

1. An increase of n for a time interval of length $O(\tau_{n(\uparrow)}) \approx \frac{1}{a_2+a_3} \ln[\frac{0.01 \cdot g(0)}{\max\{1, \frac{1}{a_5}\}}]$ (here $g \gg 100$).
2. A slow decrease of n which is governed by a sum of exponentials for a time interval of length $O(\tau_{n(\downarrow)} - \tau_{n(\uparrow)}) = O(\frac{2}{a_2+a_3} \ln[\frac{10}{\max\{1, \frac{1}{a_5}\}}])$ (here $g = O(100)$).
3. An exponential decrease of n to a_4 for a time interval of order $\ln(a_5 - 1)$ (here $g = O(1)$).

Figure 6 gives a quick graphical representation of this structure of the solutions and of the null-clines of (19) for a parameter set that we estimated from the literature (Table 1 and Section 4.1). For large g , the n null-cline asymptotes the line $n = a_4 \cdot a_5$. Thus, after an intravenous G-CSF injection, the n approaches this asymptotic value while $g(t)$ rapidly decreases from its large initial value (this takes $O(\tau_{n(\uparrow)})$ which, for typical parameter values, corresponds to around 16 hours). As g is further decreased, the neutrophils decay back to their normal values.

Noteworthy, the ability to find explicit simple formulae for the transient behavior of the system relies on the saturable form of the rate functions and not on their detailed expression. Thus, we expect similar formulae to apply to a wide variety of rate functions. Furthermore, we see that the transient time scale is mainly sensitive to the sum $a_2 + a_3$. These estimates for the duration of each of the systems' phases, derived by straightforward mathematics, have interesting medical consequences that will be further discussed towards the end of the manuscript.

4. Parameter estimation and validation

Given the prospect and the responsibility of a clinical application, the parameter estimation procedures cannot be overzealous. As an act of prudence, we estimated the model parameters by three complementary approaches: First, by a separate parameter estimation using literature reports, second by a specific fit in which certain parts of the clinical data (e.g. when $g \gg 1$) are fitted to the right-hand side of (19) and finally by making a simultaneous estimation of all the parameters by fitting detailed clinical data sets with numerical

¹⁸Recall that eventually the system returns to the stable fixed point (g^*, n^*) .

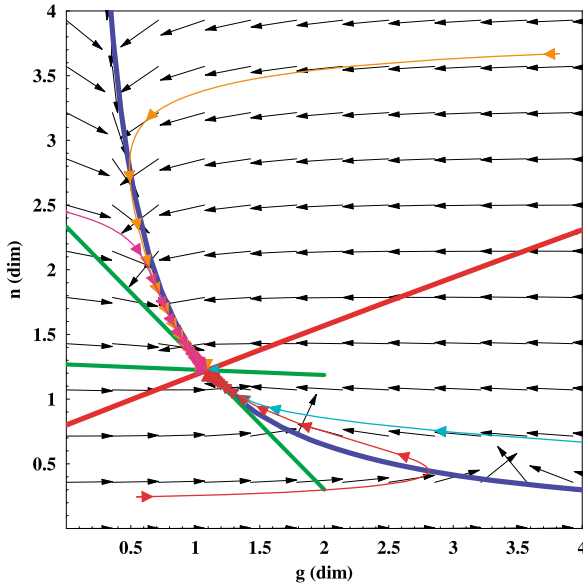


Fig. 6 Phase plane structure. The null-cline $\frac{dg}{dt} = n_1(g) = 0$ is depicted in blue. The null-cline $\frac{dn}{dt} = n_2(g) = 0$ is depicted in red. The direction field is indicated by the small black arrows. The fixed point occurs at the intersection between the two null-clines. The intersection of the null-clines is seen to be rather oblique, suggesting that the fixed point location is robust to parameter variations for the presented values. Several trajectories of the system in the vicinity of the fixed point are provided. Null-clines are drawn using the representative set of the dimensionless parameters as summarized in Table 1. The corresponding eigenvectors are depicted in green. (Colour figure online.)

solutions of the model. We end this section by examining the sensitivity of the solutions to parameter variations and by demonstrating the predictive power of the model.

4.1. Literature derived parameters

Table 1 summarizes the literature search we have conducted for evidence of the values of single parameters for the corresponding rate factors B_G , D_G , B_N , and D_N that appear in the functional terms (12–15) of the model. While we were able to preset all the model's parameters, with the majority of them from clinical human data, occasionally we needed to supplement the parameter estimation with in-vitro data as indicated in Table 1. A word of caution is in place here. Biological experiments, are typically designed to answer a specific biological question and rarely take into account the applicability of the results to mathematical modeling of medically relevant scenarios. Here, we follow the common practice by which when the values are not explicitly given they are calculated from the reported data using various biological assumptions. A typical example of such a subtle parameter is the maximal production rate of G , denoted by B_G^{\max} . To our knowledge, this value has not been intentionally measured in humans. We could though, place an upper and a lower bound for the value of B_G^{\max} by using the steady state values measured in humans and deriving the parameters from the explicit form for $f_1(G, N; \mu)$ (see Table 1). Below we provide the details for the indirect parameter estimations.

Table 1 Definition and values of model parameters used in the study. The values are estimated from the literature (“References” column)

Parameter	Meaning	Units	Value used	Possible range	Reference
B_G^{\max}	G max production rate	$\frac{\text{pgrams/ml}}{\text{day}}$	7000	$6 \times 10^3 - 2 \times 10^4$	(Ostby et al., 2003; Selig and Nothdurft, 1995) ^{a,b}
k_N	N dissociation constant	cells/ml	0.5×10^6	$(0.1-1) \times 10^6$	(Fukuda et al., 2001) ^a
k_G	G MM constant	pgrams/ml	5×10^3	$(1-5) \times 10^3$	(Wang et al., 2001) ^{d,c}
D_G^n	G elimination (by N)	$\frac{\text{pgramms/cell}}{\text{day}}$	6	3–10	(Fukuda et al., 2001; Terashi et al., 1999) ^c
D_G^r	G elimination (renal)	day^{-1}	2	1–5	(Stute et al., 1992; Terashi et al., 1999) ^c
N^*	N normal value	cells/ml	5×10^6	$(1.5-7) \times 10^6$	(Flidner et al., 2002) ^c
G^*	G normal value	pgrams/ml	30	5–100	(Selig and Nothdurft, 1995) ^c
B_N^{\min}	N min birth rate	$\frac{\text{cells/ml}}{\text{day}}$	24×10^6	$(20-40) \times 10^6$	(Joyce et al., 1976; Dancey et al., 1976) ^c
B_N^{\max}	N max birth rate	$\frac{\text{cells/ml}}{\text{day}}$	$b_N^{\min} \times 10$	$b_N^{\min} \times (8-16)$	(Wang et al., 2001; Lord et al., 1989) ^c
D_N	N death rate	day^{-1}	3	0.5–3	(Colotta et al., 1992; Mukae et al., 2000; Dancy et al., 1976; Cronkite, 1979) ^c

^aIn-vitro data

^bThe value is calculated from steady state assumptions ($f_1(\mathbf{X}; \mu) = 0$) and using G and N steady state values (Selig and Nothdurft, 1995). Noteworthy, similar estimates for B_G^{\max} where obtained by Ostby et al. (2003), from high dose chemotherapy clinical data

^cIn vivo human data

^dThe estimated k_G values represent the parameters appropriate to the specific model (see Section 4.2) and are of order 10^3 pgrams/ml. This should not be identified with the biochemical dissociation constant of G-CSF which is of order 10^6 pgrams/ml (Begley et al., 1988)

Estimation of D_G parameters: The rate of the G elimination by the kidneys and the neutrophils is estimated by using data of G-CSF clearance in lung cancer patients by Fukuda et al. (2001) (presented in Fig. 7). First we estimate the renal G-CSF clearance, Cl_G , which measures the ratio between the rate of G-CSF renal elimination and the G-CSF blood concentration¹⁹: $Cl_G = \frac{d(GV_r)}{dt} / G$ and thus $D_G^r = \frac{Cl_G}{V_d}$, where V_r and V_d are the G-CSF volume of distribution in the renal and blood ($V_d \approx 3.8$ liters Terashi et al., 1999). Alternatively (Stute et al., 1992), given $t_{1/2}$, the measured half-life of G-CSF in the blood, for low neutrophil counts the clearance is given by $Cl_G = \frac{\ln(2)}{t_{1/2}} \cdot V_d$. The effect of neutrophils as given in the parameters D_G^n and k_N is estimated by using a MM fit to the data of Fukuda et al. (2001) (Fig. 7).

Estimation of B_G parameters: The maximal rate of G influx is calculated from data by Hollenstein et al. (2000), where G-CSF kinetics was measured in healthy volunteers after LPS injections.²⁰ From Eq. (6) we take $dG/dt \approx \Delta G / \Delta t = B_G(N) - D_G$. Using the

¹⁹It is identical to the volume of blood that is entirely cleared of G-CSF per unit time ($\frac{\text{ml}}{\text{hour}}$).

²⁰LPS—lipopolysaccharide bacterial derived endotoxin which is a potent G-CSF secretion stimulator.

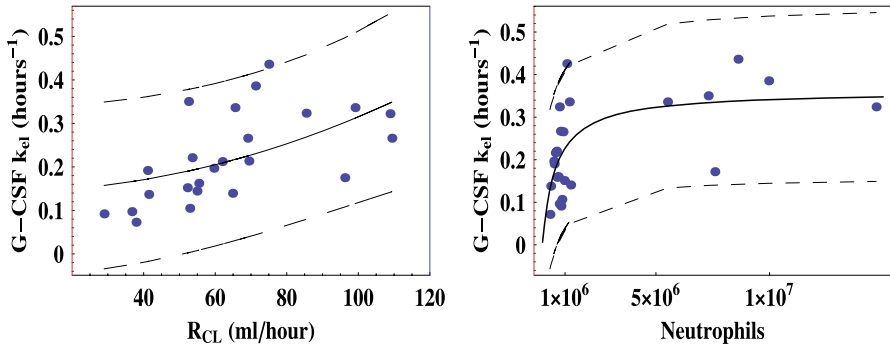


Fig. 7 The effect of renal function and neutrophil density in the blood on G-CSF elimination (adapted from Fukuda et al., 2001). Solid line displays the best fit while dashed lines denote 95% confidence intervals. G-CSF elimination parameter ($D_G^r + D_G^n$) calculated from the total G-CSF clearance, as a function of: (A) a fitted quadratic regression of renal activity R_{CL} (estimated by creatinine clearance cct): $D_G^r = 1.3 \times 10^{-5} \text{ cct}^2$. (B) a fitted *MM* function of N : $D_G^n = \frac{0.25N}{5.3 \cdot 10^5 + N}$.

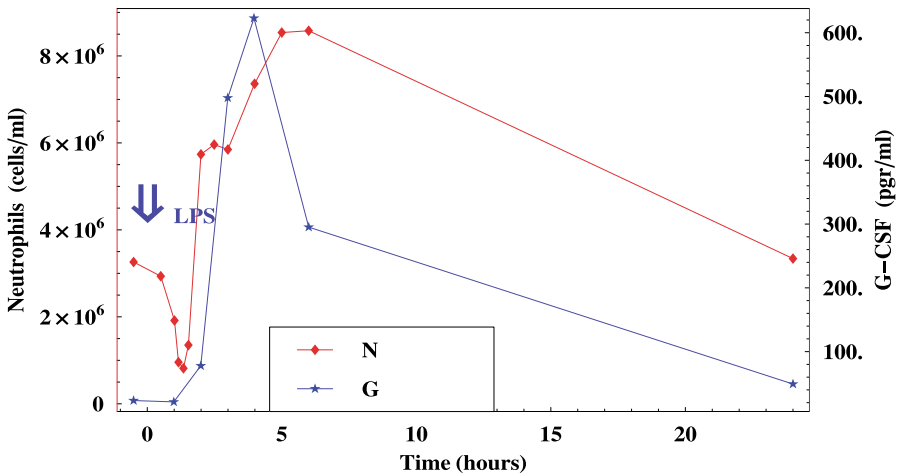


Fig. 8 G-CSF and neutrophil dynamics in healthy volunteers following single iv injection LPS (data adapted from Hollenstein et al., 2000). Observe the time course of blood neutrophils (N) (red) and G-CSF (G) (blue) following the injection. (Colour figure online.)

above calculation of D_G^r , D_G^n , k_N and using the averaged steady state value N^* , we calculate B_G^{\max} from the initial slope between hours 1 and 4 (N does not change significantly on this time scale). This gives us a lower bound of $B_G^{\max} = \Delta G / \Delta t - D_G \approx 300 \frac{\text{pgrams/ml}}{\text{hour}}$ (see Fig. 8).

We complemented the estimation of B_G^{\max} by looking at a case report by Taveira da Silva et al. (1993) about an accidental injection of very high dose of LPS. This gives an estimate for the upper bound of B_G ; $B_G^{\max} = \Delta G / \Delta t - D_G \approx 1000 \frac{\text{pgrams/ml}}{\text{hour}}$.

Estimation of B_N parameters: The influx of N at steady state is calculated from data by Dancey et al. (1976): the neutrophil kinetics was measured in normal volunteers at steady state after injections of labeled Tc (Technetium) which is incorporated into mature neutrophils before they leave the marrow. The maximal rate of N influx is calculated from data by Lord et al. (1989): an injection of labeled Tc which is incorporated into mature neutrophils before they leave the marrow, is followed by a G-CSF injection. The calculations from the flow of labeled cells to the peripheral blood indicated an addition of extra 3–4 divisions during neutrophil development.²¹

Estimation of D_N parameters: The accepted total average $t_{1/2}$ of N in the blood is estimated as 6–8 hours (Dancey et al., 1976).

4.2. Specific parameter fit

As an independent procedure, we use the asymptotic properties of the specific model (19) to fit its parameters. Here, and in Section 4.3, we use the experimental data of Wang et al. (2001). In this study, G-CSF was injected to eighteen healthy volunteers, using four different protocols on each one of them, with a 7 day intermission between the injections. Detailed results were reported for two healthy volunteers (V_a , V_b in Table 2 and the corresponding figures). The first two injections were intravenous (iv), and the G-CSF dosage was doubled on the second administration from 5 to 10 $\mu\text{g}/\text{kg}$ (which, for the averaged weight of 75 kg, is taken here as 375 μg (iv) and 750 μg (iv), respectively). The third and fourth injections with the same dosages as in the first two injections were subcutaneous (a clinically preferable mode of administration) and are not used here in the specific fit procedure since they do not produce sufficiently high peak values of g .

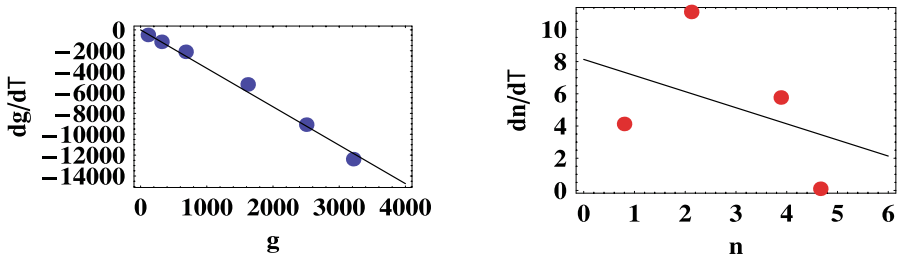
The (iv) clinical data sets are used to find the parameters as follows. First, we use the pretreatment measurements (i.e. prior to any perturbations) as the normal steady state values G^* and N^* (Table 1). From (19) and (A.2), we obtain that $a_4 \approx n^* = \frac{N^*}{10 \cdot k_N}$ and $a_1 \approx g^* \cdot a_4 \cdot (a_2 + a_3) \approx \frac{100 \cdot G^*}{k_G} \cdot \frac{N^*}{10 \cdot k_N} \cdot (a_2 + a_3)$. In general, one needs to verify that the measurement of the G-CSF level is sufficiently accurate as G^* may be below the measurement sensitivity. In the case of Wang et al. (2001), the threshold sensitivity for G is 80 pgr/ml while the typical G^* values are 30 pgr/ml as in Table 1. Hence, here, we take $G^* = 30$ pgr/ml.

To fit the other parameters, we notice that after the intravenous injections, the g values become very large,²² hence we may use the asymptotic form of (19): when $n = O(1)$ and $g \gg 1$, $\frac{dg}{d\tau} \approx -(a_2 + a_3) \cdot g$, and for $g \gg 100$, $\frac{dn}{d\tau} \approx a_4 a_5 - n \approx \frac{N^*}{10 \cdot k_N} \cdot a_5 - n$. Thus, plotting the empirical $\frac{dg}{d\tau}$ and $\frac{dn}{d\tau}$ from these data sets for the corresponding large g values (Fig. 9) provides the estimates of $a_4 \cdot a_5$ and the sum $(a_2 + a_3)$. In the plot we see that while $\frac{dg}{d\tau}$ appears to depend, as predicted, linearly on g , the dependence of $\frac{dn}{d\tau}$ on n (for large g values) does not appear to be linear as expected. This discrepancy may arise due to several different effects; first, we note that in these data sets there are only four measurements of n that correspond to large g values, and for these measurements g varies

²¹This corresponds to 2^3 – 2^4 amplification in the B_N parameter.

²²The method takes $g(0) = g_{\max}$ and is appropriate if the peak concentration is achieved very fast (which is the case for an (iv) administration). In the subcutaneous mode there is an absorption process (Wang et al., 2001) and the system becomes non-autonomous, hence it is not used for the specific parameter fit.

GivG375a \rightarrow $a_1=2.31963$; $a_2+a_3= 3.68245$; $a_4= 0.629915$; $a_5= 12.9151$



GivG375b \rightarrow $a_1=2.51966$; $a_2+a_3= 3.42343$; $a_4= 0.736003$; $a_5= 7.36747$

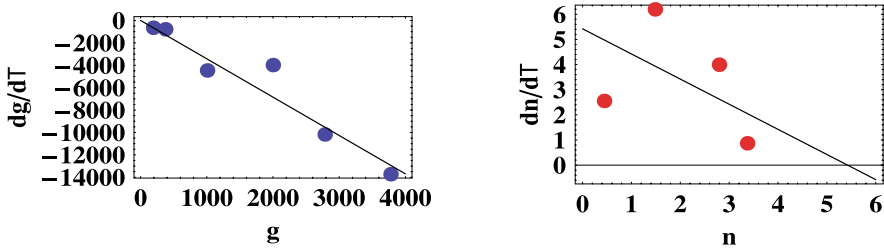


Fig. 9 Best fit (black line) of the approximated $dg/d\tau$ (only data points with $g > 10$) and $dn/d\tau$ (only data points with $g \geq 500$) to the experimentally derived G-CSF (blue dots) and neutrophil dynamics (red dots) in two healthy volunteers following single 5 $\mu\text{gr}/\text{kg}$ (iv) injection of G-CSF (data adapted from Wang et al., 2001). (Colour figure online.)

between 500–3000. Computing the term $a_4 \frac{1+0.01 \cdot a_5 \cdot g}{1+0.01 \cdot g}$ for this range of g values gives a discrepancy of $0.13a_4(a_5 - 1)$ for the constant term, namely a shift of more than a unit in the fitted line. Second, as with all experimental data, we expect that the measurement errors (which here correspond to both actual measurement errors and to natural daily fluctuations which are neglected in this model) are amplified when derivatives are taken.²³ Finally, we did not attempt to model the dynamics in the first few hours in which strong transition of the neutrophils to the extravascular space is observed (Wang et al., 2001). This strong transition might be responsible for the low value of $\frac{dn}{d\tau}$ at the very beginning of the injection process. The poor fit and the above discussion shows that the estimates of $a_4 \cdot a_5$ from the specific fit can be taken only as indicators to the order of magnitude of these parameters.

4.3. Simultaneous parameter fit

We use a χ^2 fitting procedure (normalized least-square, see Appendix A) to find the five parameters of the specific model (19) that best fit each of the above described individual data sets provided by Wang et al. (2001). In the fitting procedure we model the intravenous

²³We cannot quantify this effect from the available data since no error bars are supplied, and here, the error bars should not be identified with the variance of the full data set.

Table 2 Specific, simultaneously estimated and Literature Derived Parameter (LDV) values. Magnitude of dimensionless parameters was estimated by fitting clinical data sets (adapted from Wang et al., 2001 and Takatani et al., 1996) to the model (19). The best fit was obtained by minimizing χ^2 merit function using SVD (for the linear specific estimates) and the Nelder–Mead simplex algorithm (for simultaneous estimates) as implemented by Mathematica®

Specific parameter fit ^a	a_1	$a_2 + a_3$	a_3	a_4	a_5	v_d^b (ml)	λ_{sc}^c (1/hours)
V_a375iv	2.3	3.7	NA ^d	0.63	13	NA ^d	NA ^d
V_a750iv	3	4	NA ^d	0.74	12	NA ^d	NA ^d
V_b375iv	2.5	3.4	NA ^d	0.74	7	NA ^d	NA ^d
V_b750iv	1.9	2.3	NA ^d	0.83	9	NA ^d	NA ^d
Average_{iv}	2.4	3.4	NA^d	0.7	10	NA	NA^d
Simultaneous parameter fit ^a	a_1	a_2	a_3	a_4	a_5	v_d^b	λ_{sc}^c
V_a375iv	0.5	1.52	0.5	1.26	6	1780	NA ^d
V_a750iv	0.5	1.32	0.5	1.23	7	1528	NA ^d
V_b375iv	0.5	1.48	0.5	1	6	1558	NA ^d
V_b750iv	0.5	1.21	0.5	1.37	5	2178	NA ^d
Average_{iv}	0.5	1.38	0.5	1.21	6	1760	NA^d
V_a375sc	0.5	0.1	2.5	1	9	4000	0.17
V_a750sc	0.5	0.1	2.62	1	9	4000	0.08
V_b375sc	0.5	0.1	3.72	1	9	3874	0.13
V_b750sc	0.5	0.1	5	1	9	1610 ^e	0.09
Average_{sc}	0.5	0.1	3.46	1	9	3960^e	0.11
<i>LDV range</i>	4–400	0.33–10	1–20	0.66–80	8–16	NA ^d	NA ^d
<i>LDV-value used</i>	4.66	0.66	2	1.6	8	1800 (Wang et al., 2001)	0.3 (Wang et al., 2001)

^aThe values are rounded to the first decimal digit

^b v_d is the volume of G-CSF distribution following injection (ml)

^c λ_{sc} is the (sc) influx parameter

^dNot applicable. *LDV* Literature derived values are calculated by using the appropriate biological parameters presented in Table 1

^eThe initial G-CSF profile resembles (iv) injection rather than s.c. (excluded from average)

and the subcutaneous injections as two different types of source terms, in $G(t)$, in the G equation. For the intravenous injections, we take:

$$in_{iv} G(t) = \begin{cases} \frac{dose_G}{v_d} & \text{for } t \in [0, t_{in}], \\ 0 & \text{otherwise.} \end{cases}$$

The parameters $dose_G$ and t_{in} are given ($t_{in} = 30$ min and $dose_G = 375, 750 \mu\text{gr}$ in the first two sets). The volume of distribution V_d that was estimated indirectly by Wang et al. was also fitted (as a sixth parameter) in our fitting procedure. For the subcutaneous injections, the G-CSF is distributed to the blood by passive diffusion from the subcutaneous site

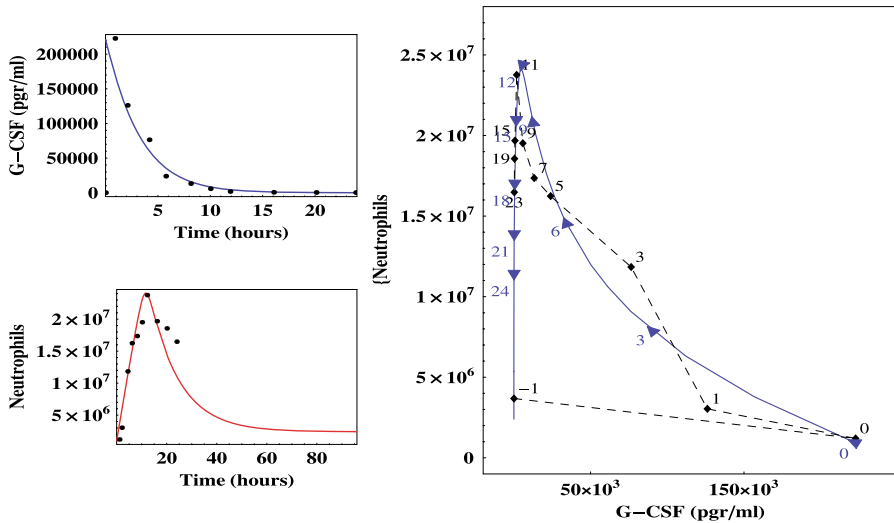


Fig. 10 Experimental (black dots) and simulated G-CSF (blue line) and neutrophil dynamics (red line) in healthy volunteers following single (iv) injection of G-CSF (data adapted from Wang et al., 2001). The right figure gives the experimental (dashed) and the simulated full (blue solid) and concise (blue dashed) phase portraits of the dynamics. Numbers denote the time course of the trajectory. (Colour figure online.)

(Wang et al., 2001; Shochat and Stemmer, 2002), so a first order kinetics influx from the subcutaneous deposit was assumed:

$$\text{in } G(t) = \lambda_{\text{sc}} \frac{\text{fb}_G \text{dose}_G}{V_d} e^{-\lambda_{\text{sc}} t}$$

where $\text{fb}_G \approx 0.7$ is the subcutaneous G-CSF bioavailability (Wang et al., 2001), $\text{dose}_G^i = 375, 750 \mu\text{gr}$ are again the injected doses, and λ_{sc} is the (dimensional) influx parameter. Thus, in this case the two additional parameters λ_{sc} and V_d are added to the fitting procedure. The results of the parameter fit (within two significant digits), using a χ^2 merit function for the G-CSF and the neutrophils data sets,²⁴ is presented in Table 2 and by the solid curves in Figs. 10 to 14. The resulting values of the dimensionless parameters together with the dimensionless version of Table 1 are presented below.

From the limited data set (only two patients), we cannot conclude whether patient's variability is significant. We do note a significant change in the parameters corresponding to the two different methods of G-CSF administration (and, possibly, with the number of injections which were administered). While formally we should not observe such a parameter dependence on the form of the administration, the actual discrepancies may be explained by realizing that each clinical scenario embraces only a part of the possible dynamics embedded in the full model. For example, when the G-CSF is administered directly to the blood, its influx overwhelms any potential addition that the endogenous

²⁴As the initial values of G-CSF are below the measurement threshold (Wang et al., 2001), for the simulation in all the figures these were taken at the fixed point values.

production represented by a_1 can achieve. Thus, all the simultaneous estimations are insensitive to a_1 , and it is best estimated by the specific fit which works well only for the intravenous protocol. Simultaneous estimation may also underestimate the neutrophil's clearance rate for normal neutrophil's concentrations as G-CSF is mixed almost instantaneously and renal clearance acts on G-CSF prior to the neutrophil's clearance (so a_2 is three times larger than a_3). On the other hand, when the G-CSF is administered by a subcutaneous injection, it slowly diffuses to the blood, and just then to the renal region, and thus there exists a transient period at which the neutrophils have a longer time to act, leading to larger a_3 value. Notice that in the simultaneous fit the overall value of $a_2 + a_3$ is slightly larger than its value in the subcutaneous injection case. The analysis and the clinical implications of the form of the G-CSF administration are under current study.

4.4. Chemotherapy data set fit

So far, we modeled physiological data sets and the GN dynamics after G-CSF injections. Can our model capture the GN dynamics following a chemotherapy insult? As Fig. 2A shows, following a chemotherapy treatment a brisk neutropenia is ensued which is promptly followed by approximately 10 fold increase of intrinsic G-CSF and then an eventual recovery in neutrophils. Based on the sensitivity analysis (see next subsection), we hypothesize that a chemotherapy insult may be modeled by a temporary substantial decrease of a single parameter: the background marrow proliferation capacity a_4 , which corresponds to the background neutrophils influx to the blood (the B_N^{\min} parameter). We observe that this single hypothesis is sufficient to reproduce the data (Fig. 11). The validity and implications of this hypothesis are under current study.

4.5. Model sensitivity

Asymptotically, all the solutions of (19) converge exponentially to the unique fixed point. The dependence of the fixed point on the parameters is studied analytically in the appendix; It is shown that both g^* and n^* depend monotonically on each one of the non-dimensional parameters a_{1-5} . Hence, the extreme values of g^* , n^* are achieved on the extreme points of the parameters domain. Fixing the parameters to the fitted values and varying one parameter at a time between its minimal to its maximal value, shows that even though $g^*(a_i)$ may vary by up to two orders of magnitude at a time, $n^*(a_i)$ is extremely robust to variations of $a_{1,2,3,5}$ ²⁵ while variations of a_4 change n^* significantly²⁶ (see also Fig. 12).

Indeed, it is shown in the appendix that for typical parameter values $\frac{\partial n^*(a)}{\partial a_4} \approx 1 \gg \frac{\partial n^*(a)}{\partial a_j} = O(0.01)$ for $j = 1, 2, 3, 5$.

From the clinical point of view, this result emphasizes that B_N^{\min} and D_N are the *only* parameters that may significantly influence the neutrophils equilibrium point N^* . We have seen that the transient behavior for the considered cases $(n(0), g(0)) = O(1, 10^3)$ is governed by two main effects: the maximal value of n is approximately given by $a_4 a_5 = \frac{1}{10 \cdot k_N} \frac{B_N^{\max}}{D_N}$ and the time scale for returning to the neighborhood of the fixed point

²⁵ $n^*(a_i) \in (1.2, 3.5)$ for $i = 1, 2, 3, 5$.

²⁶ Recall that $n^* \approx a_4$.

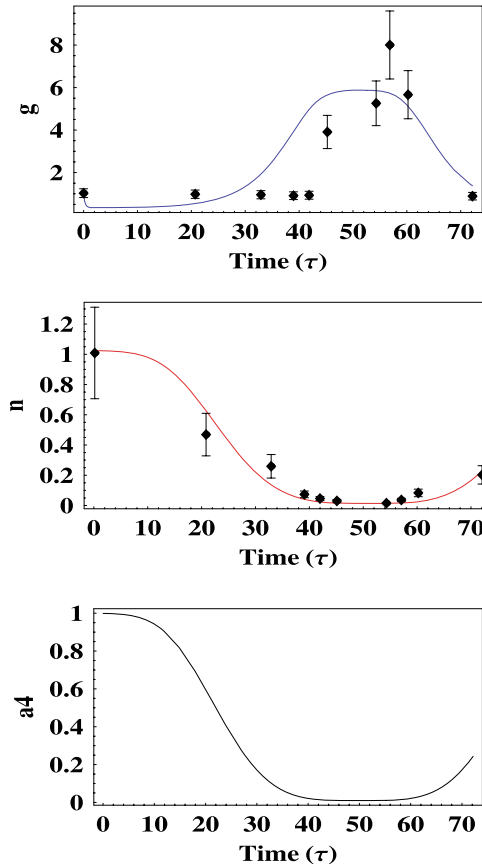


Fig. 11 Bone marrow regeneration dynamics following HDCT in children with hematological malignancies (data as in Fig. 2B is adapted from Saito et al., 1999). (A, B) G-CSF (G) and neutrophil (N) dynamics labeled blue and red, respectively. Note the threshold neutrophil level of $0.1 \approx 500 \times 10^3$ cells/ml which triggers prompt increase in G-CSF levels. (C) Best fit for time dependent $a_4(t) = a_4(0) \cdot (1 - e^{-\alpha(t-\beta)^4})$ where $\alpha = 10^{-6}$ and $\beta = 50$ are schedule dependant. The remaining parameters are fixed at the following values: $a_1 = 2$; $a_2 = 2$; $a_3 = 2$; $a_4(0) = 1$; $a_5 = 8$. (Colour figure online.)

is of order of $\frac{1}{a_2+a_3} \ln g(0) + \ln(a_5 - 1)$, so the “area under curve” is proportional to $a_4 a_5 (\frac{1}{a_2+a_3} \ln g(0) + \ln(a_5 - 1) + C)$. Thus, while doubling the production of neutrophils by $a_4 a_5$ doubles this area, doubling the dose of g only increases this area by $\frac{a_4 a_5}{a_2+a_3} \ln 2$ (which, for the a_{iv} values is 2.6767 and for the a_{sc} values is 1.75). This simple calculation explains the clinical observation that often pulsed G-CSF therapy by injection cannot fully counteract the chemotherapy induced depletion of a_4 .

We note that parameter estimation is a crucial step in convergence to a clinically applicable model. Our analysis shows that literature derived parameters may vary significantly from the best fit parameters that are estimated simultaneously from specifically dedicated data. Literature search is a valuable process for generating ideas during

Sensitivity analysis N

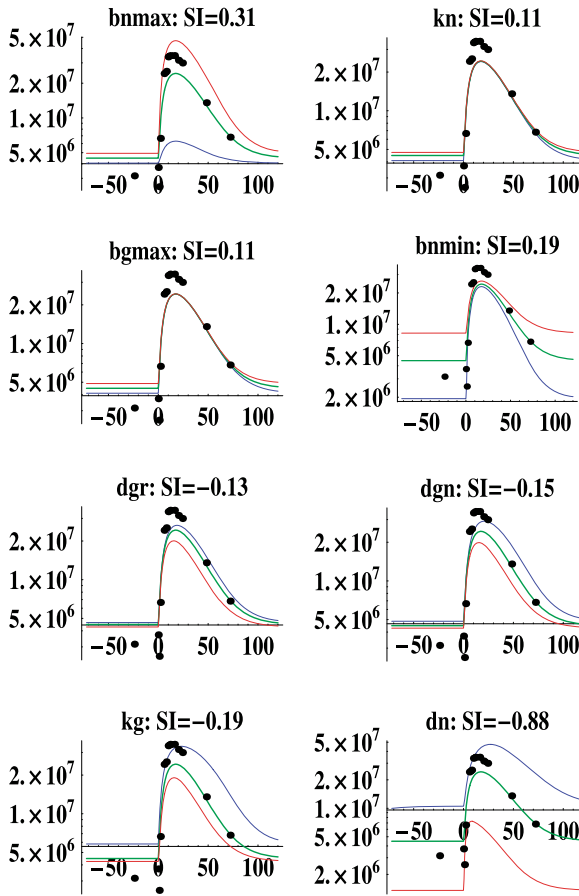


Fig. 12 Sensitivity of the transient dynamics to variation in the individual parameters. Each curve is a linear–log scaled dynamics of neutrophils following G-CSF injection indexed by the parameter name and the corresponding sensitivity index SI. The sensitivity index $SI = \text{sign}(AUC(\mu_i^{\max}) - AUC(\mu_i^{\min})) \frac{AUC(\mu_i^{\max})/AUC(\mu_i^{\min})}{\mu_i^{\max}/\mu_i^{\min}}$ where AUC is the area under the trajectory curve. Note that $|SI| > 1$ reflects high (non-linear) sensitivity while $|SI| \approx 0$ corresponds to low sensitivity. Black points denotes experimental counts (adapted from Wang et al., 2001).

model development and for obtaining the relevant range of parameters. Since our literature search involved many different experimental settings and indirect estimates it produced a large range of the parameters, with no good indication on what is the appropriate set of typical parameter values. Indeed, the best fit to the present model was achieved by using the reported data from pharmacological experiment that was pre-designed with modeling in mind (Wang et al., 2001).

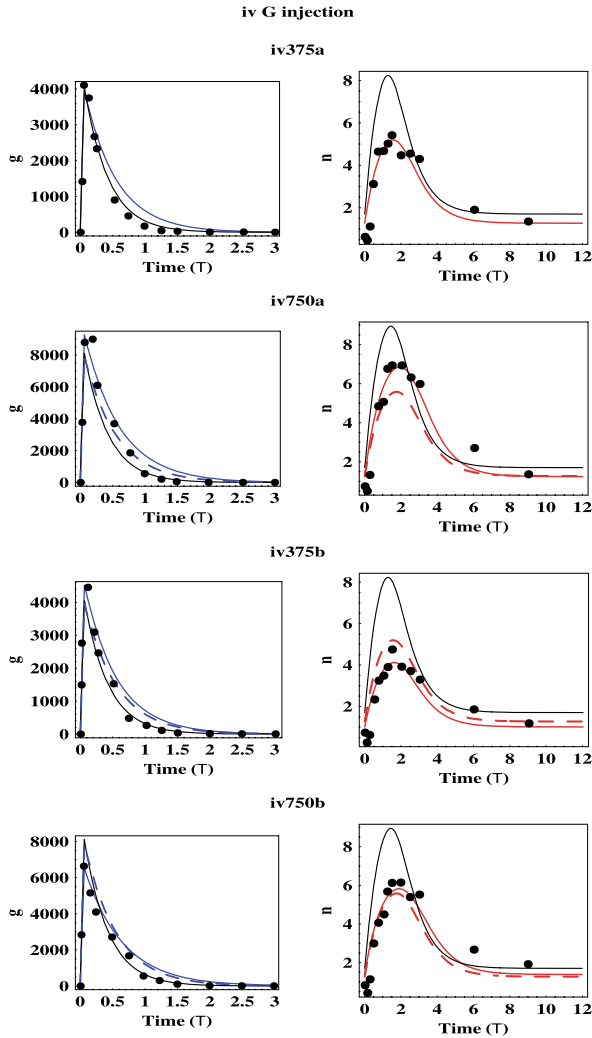


Fig. 13 Predicting the GN dynamics following an (iv) injection by the parameterized model. Experimental (black dots), the individual best fit curves (colored solid lines) and predicted curves (dashed lines) of G-CSF (blue) and neutrophil (red) dynamics in two healthy volunteers following a single (iv) injection of G-CSF (375 $\mu\text{g}/\text{kg}$ and 750 $\mu\text{g}/\text{kg}$ sc). The predictions (dashed lines) in all the figures were generated by using the parameter fit for the first injection to the first patient only (upper figure ivc375a). Data adapted from Wang et al. (2001). Black solid lines indicate simulations based on literature derived parameters. (Colour figure online.)

4.6. Model validation

To assess the ability of the fully parameterized model to *predict* possible manifestations of the GN dynamics we use the parameter fits of the first (iv) (intravenous) injection and first (sc) (subcutaneous) injection to predict the behavior of all other cases (i.e. to predict

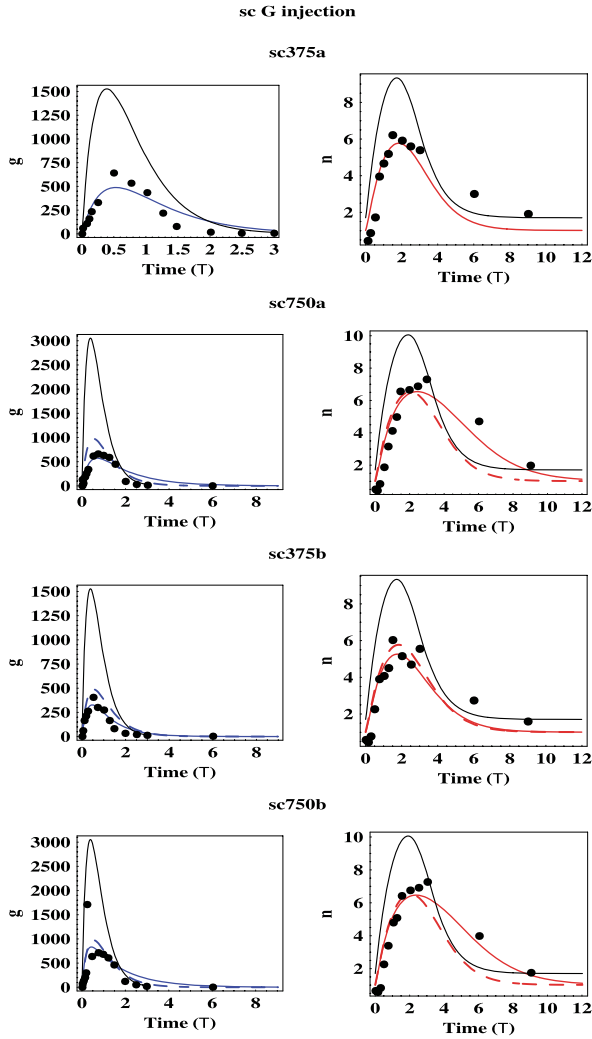


Fig. 14 Predicting the GN dynamics after a (sc) injection by the parameterized model. Experimental (black dots), the individual best fit curves (colored solid lines) and predicted curves (dashed lines) of G-CSF (blue) and neutrophil (red) dynamics in two healthy volunteers following a single (sc) injection of G-CSF (375 $\mu\text{g}/\text{kg}$ and 750 $\mu\text{g}/\text{kg}$ sc). The predictions (dashed lines) in all figures were generated by using the parameter fit for the first injection to the first patient only (upper figure sc375a). Data adapted from Wang et al. (2001). Black solid lines indicate simulations based on literature derived parameters. (Colour figure online.)

the GN dynamics of the first volunteer after doubling the dosage and to predict the GN dynamics of the other volunteer after each one of the two injections). The results of the predictions are shown as the dashed lines in Fig. 13 for the (iv) case, and in Fig. 14 for the (sc) case. We stress that *these dashed lines are drawn with no parameter fitting at all*. In particular, our *prediction*, that at these values of g , doubling the dosage of g hardly

changes the dynamics in n are thus confirmed. Although the preliminary results appear promising, clearly, a large cohort of patients data is needed to better assess both the validity of the specific functional form and whether a dedicated fitting in individual patients is in place.

Furthermore, notice that the results in Table 2 support the assertion that our model captures the essential features of the GN dynamics. Indeed, the parameter values found for the four distinct injections for the two different patients and the fitting of a different patient undergoing chemotherapy are all very similar (thus, choosing a different training set in Figs. 13 and 14 produces similar results). Notice that a_5 is the only parameter which is changing to leading order under subsequent injections. These changes in a_5 may reflect the saturable effect of multiple G-CSF injections on the bone marrow proliferation which can be clinically observed (Pollmacher et al., 1996).

5. Conclusion

We constructed a two-dimensional system describing the G-CSF neutrophil dynamics. The model is defined by generic biological properties (7–9) that are deduced from clinical observations. We proved that this general model has the observed asymptotic behavior—a robust, stable, positive equilibrium point. The existence and the stability of the fixed point emerged as a consequence of the axiomatic construction of the model rather than an a priori assumption (such as introducing a logistic term). We concluded that since this behavior is structurally stable, our model will be robust to small inaccuracies in the exact modeling procedure. *The structural stability of the mathematical model fits well the clinically observed robustness of the GN dynamics.* We provided explicit functional form for the model, containing five dimensionless parameters. We demonstrated that these parameters may be fitted from data set of a response to a single G-CSF injection. We demonstrated that the fitted model supplies good predictions for subsequent G-CSF injections. Finally, we demonstrated that the current model suffices for *predicting the neutrophils dynamics on a time scale of several days*. The intentional restriction to this limited time scale allows to construct a simple model with a low number of parameters that may be directly estimated from relatively limited clinical data. Thus, the clinical approximation that relegates a dominant role to G-CSF is expected to be valid only on the several days time scale in which the model's parameters may be considered as constant. Noteworthy, this intermediate time scale appears to be relevant in treating neutropenia (see Figs. 4, 2B).

6. Discussion

6.1. Methodology

A possible criticism of low dimensional models is that these intentionally neglect some effects of other variables that may influence the dynamics in an uncontrolled fashion. Here, the axiomatic construction of the GN system leads to a structurally stable dynamics (which reflects, admittedly, that the underlying dynamics is rather simple and low dimensional). Furthermore, the intentionally neglected variables (i.e. the bone marrow

and the bacteria) typically vary on time scales that are well separated from the GN typical time scales; the bone marrow varies much slower than the GN (Fig. 2B), whereas the bacteria varies much faster (Fig. 8). Hence, for time scales on which the bone marrow dynamics may be taken as constant (3–5 days under normal conditions) and under the assumption that the infectious stimulus quickly adjusts to a bounded (as is the case in a healthy person) quasi-steady state, our model still applies. One issue which we have not addressed explicitly is the interaction between the tissue and the blood concentrations of the neutrophils and the G-CSF. Indeed, we have seen that with the current model the fitted value of the sum of the renal and neutrophil clearance rate $a_2 + a_3$ and their ratio a_2/a_3 appears to depend on the G-CSF administration procedure (see Section 4.3). Furthermore, in formulating the axiomatic observations regarding the form of $D_N(G)$ (which has a component of migration of the neutrophils from the blood to the tissue) we encountered conflicting phenomenon which may potentially be resolved by a compartmental model (see Fig. 9). Thus, understanding the role of the neutrophils consumption of G-CSF in the tissue versus its consumption in the blood, which is especially relevant for the infection related time scales of the first few hours following an infection, requires additional study.

This conclusion demonstrates the ability of the axiomatically constructed model to detect inconsistencies in some working hypotheses regarding the GN dynamics, and enables us to examine at which instances the biological hypothesis that are put into the model fail. Such examples appear when one attempts to apply the GN model to situations, such as cyclical neutropenia, where the neutrophil level oscillates on a time scale of about 21–28 days. This rare behavior, of stable large amplitude periodic motion, cannot appear in the two-dimensional system defined by the hypothesis listed in Section 2. Thus, either the system is not two-dimensional or the assumptions on the form of the rate functions are not exact. To the best of our knowledge, in this condition, the assumptions on the form of the rate functions still hold. Thus, we can suggest that in the case of cyclic neutropenia, higher dimensional model must be introduced. For example, to get a periodic solution in our model, we may introduce periodic a_4 , which reflects periodic dynamics in the bone marrow. Noteworthy, the extensive studies of cyclic neutropenia in the last three decades using delayed differential equations models²⁷ (Bernard et al., 2003; Foley et al., 2006; Haurie et al., 2000), concluded that a disorder in the bone marrow compartment (an additional variable in our framework) must be introduced to obtain cyclic behavior.

Such effects of the long term dynamics can be introduced by extensions to higher dimensional models.²⁸ The time scales involved in these phenomena are well separated from the GN dynamics studied here. Hence, we expect that the stable fixed point that is obtained in the current two-dimensional model will appear as an attracting sub-manifold of the higher dimensional system, and that on this sub-manifold slower dynamics will develop. From the biological perspective, while in our model the parameters that govern the production of the neutrophils in the bone marrow are fixed, in reality, these parameters

²⁷In these models the G-CSF effects are implicitly introduced as a delayed negative feedback on the neutrophil production and the bone marrow activity is introduced as a periodic forcing (Haurie et al., 2000) or as an additional variable (Foley et al., 2006).

²⁸A numerical investigation of high ODE dimensional system (60 ODE equations), which encompassed many of these effects, indeed tracks the long term behavior (several months) of the bone marrow following transplant, and of the properties of very early stem cells (Shochat and Stemmer, 2002). In contrast, the two-dimensional system models transient dynamics on time scales of several days only.

may vary slowly via complex (indirect) and sometimes poorly understood mechanisms that depend on the chemotherapy effects, G-CSF levels, and other cytokines that were not explicitly introduced and that act through intermediate progenitors of the neutrophils (Ratajczak and Gewirtz, 1995; Bronchud et al., 1988; Moore, 1991). In particular, some of the G-CSF activity has a delayed effect that surfaces several days and even weeks after the actual administration²⁹ (Pollmacher et al., 1996).

Next, we outline some possible applications of the *present model* to specific clinical situations.

6.2. Medical implications

We propose to apply the simple two-dimensional model presented here to clinical situations in which the parameters of the production and death rates of the neutrophils and the G-CSF are approximately constant or change very slowly relative to our typical scale of 3–5 days. First, we suggest to view the normal physiology as corresponding to the behavior of the system with typical parameters near the normal stable fixed point. In this context, the various clinical situations (i.e. a disease or a drug treatment) will correspond to either a perturbation in the initial conditions, a change in the parameter values, a modulation of these parameters in time or a combination of all these effects. Consider the parameter list as given in Table 1 and the possible (positive and negative) alterations in their values. We identified a list of clinical situations where specific alterations of parameters may indeed take place (Table 3). We then looked at the effect of parameter perturbation on the G^* , N^* steady state values as predicted by the model (by looking at the sign of $\frac{\partial x^*(a)}{\partial a_j}$ for $x = G, N$ and $j = 1 - 5$) and compared them with the G^* , N^* values reported for these conditions.³⁰ The trend that is observed in the clinic regarding the changes in the normal fixed point values matches the model predictions when the appropriate trend of the parameters is entered.

A detailed discussion of the dynamics in each of these cases and the specific correspondence to the clinical data may be the scope of further studies. We briefly discuss two of the interesting observations that emerge from the analysis:

1. The first observation concerns a possible mechanism of highly increased value of neutrophils steady state N^* observed in chronic myeloid leukemia (CML) (Thiele and Kvasnicka, 2002). We have previously shown that under plausible conditions

$$g^* \approx \frac{a_1}{a_4(a_2 + a_3)}, \quad n^* \approx a_4. \quad (21)$$

It follows that the increased N^* values in CML may correspond to a significantly increased a_4 , which can be achieved by either an increase in B_N^{\min} OR a decrease in³¹ D_N , and both phenomena can be observed in the clinic (Table 3). Indeed, the recent dramatic success in CML treatment with the drug Glivec (Imatinib) is contributed to the very strong inhibition of stem cell proliferation by the drug (Marley and Gordon, 2005).

²⁹This may explain the change in a_5 in the consequent injections as observed in Table 2.

³⁰The estimates (20) for the fixed points were performed under the conditions derived in (A.1) in Appendix A.1.

³¹Notice that the latter changes $a_{1,2,3}$ as well, but the sensitivity to these is small.

Table 3 Parameters perturbation and the plausible corresponding clinical conditions

Parameter	Model prediction	Clinical condition	Observation ^{a,b}
$B_G^{\max} \downarrow$	$\frac{\partial G^*}{\partial B_G^{\max}} > 0 \checkmark$	Septic shock	$G^* \downarrow$ (Weiss et al., 2003)
$D_G^r \downarrow$	$\frac{\partial G^*}{\partial D_G^r} < 0 \checkmark$	Renal failure	$G^* \uparrow^c$ (Wen et al., 2001)
$D_G^r \& D_G^n \downarrow$	$\frac{\partial G^*}{\partial D_G^n} < 0 \checkmark$	Pegfilgrastim	$G^* \uparrow$ (Molineux, 2003; Kotto-Kome et al., 2004)
$B_N^{\min}(\varepsilon\tau) \downarrow$	$\frac{\partial G^*}{\partial B_N^{\min}} < 0, \frac{\partial N^*}{\partial B_N^{\min}} > 0 \checkmark$	Neutropenia	$G^*(\varepsilon\tau) \uparrow N^*(\varepsilon\tau) \downarrow$
$\frac{B_N^{\max}}{B_N^{\min}}(\varepsilon\tau) \downarrow$	$\frac{\partial G^*}{\partial a_5} < 0, \frac{\partial N^*}{\partial a_5} > 0 \checkmark$	(Chemotherapy induced)	(Fliedner et al., 2002; Shochat and Stemmer, 2002; Takatani et al., 1996)
$B_N^{\min} \uparrow$	$\frac{\partial N^*}{\partial B_N^{\min}} > 0 \checkmark$	CML ^d	$N^* \uparrow$ (Thiele and Kvasnicka, 2002)
$k_g \uparrow$	$\frac{\partial N^*}{\partial k_g} < 0 \checkmark$	Myelodysplastic syndrome	$N^* \downarrow$ (Kimura and Sultana, 2004)
$D_N \downarrow$	$\frac{\partial N^*}{\partial D_N} \approx -\frac{\partial n^*}{\partial a_4} < 0 \checkmark$	CML	$N^* \uparrow$ (Gisslinger et al., 1997)
$G(0) \uparrow$	\checkmark	G-CSF external injection	$G \uparrow \& N \uparrow$ (Wang et al., 2001)
$N(0) \uparrow$	\checkmark	Neutrophil infusions ^e	$N \uparrow$ (Price et al., 2000)

^aMeasurable effect on G_* and N_* relative to the normal values provided in Table 1

^bReferences quote the articles that suggest a relevance of the parameter alteration in question to the clinical problem

^cThe $G_* \approx 380$ value predicted by solving the steady state model are comparable with G-CSF provided in (Wen et al., 2001) ($G \approx 560$)

^dCML = Chronic myeloid leukemia

^eMostly applicable in hematological setting of stem cell transplantation. The perturbations of parameters that are analyzed in this study are marked in bold. See Appendix A for the derivatives computation

2. The second observation concerns a potential enhancement of G-CSF activity, by keeping $(a_2 + a_3) \ll 1$. Then, it follows that $g^* \approx \frac{a_1}{0.1a_2 + a_4a_5(a_2 + a_3)} + O(1)$ and $n^* \approx a_4a_5$, hence, a significant increase of the neutrophils levels may be achieved when *both* consumptions rates (D_G^r and D_G^n)³² are kept low. Notice that a decrease in $a_2 + a_3$ also increases the transient time of the decay of $g(0)$, and thus the “area under curve” which is proportional to $a_4a_5(\frac{1}{a_2 + a_3} \ln g(0) + \ln(a_5 - 1) + C)$. In particular, we see that changing the parameters $a_2 + a_3$ is significantly more efficient than increasing the dosage of the G-CSF and thereby altering $g(0)$. Indeed, with this motivation in mind, a new form of therapeutic G-CSF (pegylated G-CSF) with double the molecular weight of the regular version, was developed and has been recently put into clinical use (Table 3).

Finally, our motivation to study GN dynamics stems from a practical need to explore new potential utilization of G-CSF to reduce the nadir duration and subsequently the risk of neutropenic fever in cancer patients. We have shown that neutrophil dynamics can be effectively represented by two-dimensional model in cases in which the model’s

³²An alternative route is an increase in D_N with a corresponding increase in B_N^{\max} which, to our knowledge, does not correspond to any known biological feature.

parameters are relatively constant. Our analysis suggests that the chemotherapy effect is accompanied by a significant time dependent changes in a_4 parameter (Fig. 11). The next challenge may be to look for the minimal expansion that will adequately introduce a chemotherapeutic effect into the model while maintaining the effective simplicity of representation. Such a model that takes into consideration the trade off between the details and the clinical applicability is currently being developed.

Acknowledgements

We thank Edriss Titi, Anna Rapoport, Philip Holmes, and Solomon Stemmer for stimulating and detailed discussions. We thank Boaz Nadler, Michael Grinfeld and Leah Edelstein-Keshet for their careful reading and insightful comments of this manuscript. We thank the Minerva foundation for its financial support.

Appendix A

A.1 Fixed point analysis

Computing the null-clines explicitly for (19) we get:

$$n_1(g) = \frac{1}{g} \frac{a_1}{a_2 + a_3} - \frac{0.1 a_2}{a_2 + a_3}, \quad n_2(g) = a_4 \frac{1 + a_5 \cdot 0.01 \cdot g}{1 + 0.01 g}. \tag{A.1}$$

In particular, we see that for sufficiently small g , $n_1(g) > n_2(g)$, whereas at $g = 10 \frac{a_1}{a_2}$, $n_1(g) = 0 < n_2(g)$, hence, by Theorem 2.1, the system always has a stable fixed point (n^*, g^*) with $g^* \in (0, 10 \frac{a_1}{a_2})$. Indeed, the explicit solution of the quadratic equation for g^* , which is found from the null-cline intersection point: $n_1(g^*) = n_2(g^*)$, shows that the equation has only one solution in the positive quadrant:

$$\begin{aligned} g^* &= \frac{-100(a_4(a_2 + a_3) + 0.1a_2 - 0.01a_1)}{2(a_4a_5(a_2 + a_3) + 0.1 a_2)} \\ &\quad + 100 \frac{\sqrt{(a_4(a_2 + a_3) + 0.1a_2 - 0.01a_1)^2 + 0.04(a_4 \cdot a_5(a_2 + a_3) + 0.1 a_2)a_1}}{2(a_4a_5(a_2 + a_3) + 0.1 a_2)} \\ &= \frac{50}{a_5} \left(-1 + \sqrt{1 + \frac{0.04 \cdot a_5 a_1}{a_4(a_2 + a_3)}} + O\left(\frac{0.1a_2 + 0.01a_1}{a_4a_5(a_2 + a_3)}\right) \right) \\ &= \frac{a_1}{a_4(a_2 + a_3)} \left(1 + O\left(\frac{1}{a_5^2}\right) \right). \end{aligned}$$

The trace and determinant of the linearized matrix, and thus the eigenvalues, are similarly approximated (with the additional assumption $0.1 \ll a_4$):

$$\text{trace}(\mathbf{J}) = -\left(a_2 + \frac{a_3 \cdot n^*}{n^* + 0.1}\right) - 1 \approx -(a_2 + a_3) - 1,$$

$$\det J = \frac{1}{g} \frac{a_1}{n + 0.1} + a_4 \frac{(a_2 + a_3) \cdot g}{n + 0.1} \frac{0.01 \cdot (a_5 - 1)}{(1 + 0.01g)^2} \approx (a_2 + a_3),$$

$$\kappa = 4 \frac{\det(J)}{\text{trace}^2(J)} \approx 4 \frac{a_2 + a_3}{((a_2 + a_3) + 1)^2},$$

$$\lambda = \frac{\text{trace}(J)}{2} (1 \pm \sqrt{1 - \kappa}) \approx \{-(a_2 + a_3), -1\},$$

where the approximations are valid provided:

$$\frac{0.1a_2 + 0.01a_1}{a_4(a_2 + a_3)}, \frac{0.04 \cdot a_5 a_1}{a_4(a_2 + a_3)}, \frac{1}{a_5^2} \ll 1.$$

Hence, under these conditions we see that

$$g^* \approx \frac{a_1}{a_4(a_2 + a_3)}, \quad n^* \approx a_4, \tag{A.2}$$

and the eigenvalues are approximately $\{-(a_2 + a_3), -1\}$. These conditions are satisfied under normal physiological circumstances. On the other hand, if $(a_2 + a_3) \ll 1$ then $g^* \approx \frac{a_1}{0.1a_2 + a_4a_5(a_2 + a_3)} + O(1)$ and $n^* \approx a_4a_5$, hence, a significant enhancement of the neutrophils may be achieved provided *both* consumption rates are kept law.

More generally, we see that the null-cline $n_1(g)$ becomes nearly parallel to the g axis for large g and to the n axis for small³³ g . It follows that the robustness in n is lost if for some parameter values $g^* \ll 1$ and the robustness in g is lost if $g^* \gg 1$. The conditions under which these two extreme possibilities may be realized and their clinical interpretation will be a subject of future study (see also discussion section).

A.2 Asymptotic form

For large g values and n values that are not too small (e.g. following an injection of G-CSF in healthy volunteers), the transient behavior of the system may be estimated analytically; if $n \gg 0.1$ and $g \gg \frac{1}{(a_2 + a_3)}$, it follows from (19) that g may be approximated by

$$g^{as}(\tau) = g(0)e^{-(a_2 + a_3)\tau}. \tag{A.3}$$

The corresponding n behavior is extracted from (19) by integrating $\frac{dn}{d\tau} \approx a_4 \frac{1 + 0.01a_5 \cdot g^{as}(\tau)}{1 + 0.01g^{as}(\tau)} - n$. For large g values ($g \gg 100 \max\{1, \frac{1}{a_5}\}$) this yields $\frac{dn}{d\tau} \approx a_4a_5 - n$ so that

$$n(\tau) \approx a_4 \cdot a_5(1 - e^{-\tau}) + n(0) \cdot e^{-\tau}, \tag{A.4}$$

³³Note that for $g \ll 1$, $|\frac{dn_1(g)}{dg}| \gg 1$ and $\frac{dn_2(g)}{dg} \approx 0.01 \cdot a_4 \cdot a_5$ while for large g , both $|\frac{dn_1(g)}{dg}|$ and $|\frac{dn_2(g)}{dg}| \ll 1$.

Table A.1 Sensitivity of the fixed point (g^*, n^*) to fluctuations in the parameters. Minimal and maximal values of $g, n, n_{a_j}^* - g, n_{a_j}^{*\max}$ for each varied dimensionless parameter a_j (while fixing all others to an average value) are presented. The parameter range is reported in Table 2

	$g_{a_j}^* - g_{a_j}^{*\max}$	$n_{a_j}^* - n_{a_j}^{*\max}$
a_1	0.20–60	1.22–3.48
a_2	0.47–0.04	1.24–1.21
a_3	0.2–0.02	1.22–1.21
a_4	0.35–0.003	0.67–80.0
a_5	0.205–0.201	1.22–1.24

and in particular, if $n(0) < a_4 \cdot a_5$, n increases exponentially (denoted as $n(\uparrow)$) till the nullcline $(g, n_2(g))$ is reached. For relevant clinical values of the parameters,³⁴ this exponential increase of n lasts for $\tau_{n(\uparrow)} \approx \frac{1}{a_2+a_3} \ln\left[\frac{0.01 \cdot g(0)}{\max\{1, \frac{1}{a_5}\}}\right]$ (about 16 hours).

When $g(\tau)$ is of order one ($g \ll 100 \cdot \max\{1, \frac{1}{a_5}\}$), so $\tau \approx \tau_{n(\downarrow)} = \frac{1}{a_2+a_3} \log g(0)$, the equation for n becomes $\frac{dn}{d\tau} \approx a_4 - n$, so n decreases exponentially from its approximate maximal value of $a_4 \cdot a_5$ as $a_4 + a_4(a_5 - 1)e^{-(\tau - \tau_{n(\downarrow)})}$ (recall that these approximations are valid as long as $n \gg 0.1, \frac{a_1}{(a_2+a_3)g}$, i.e. as long as $a_4 \gg 0.1$).

It follows that the transient time, at which n slowly decreases from its near maximal value to the region at which it decreases exponentially is given by:

$$\begin{aligned} \tau_{n(\downarrow)} - \tau_{n(\uparrow)} &\approx \frac{1}{a_2 + a_3} \log g(0) - \frac{1}{a_2 + a_3} \ln\left[\frac{0.01 \cdot g(0)}{\max\{1, \frac{1}{a_5}\}}\right] \\ &\approx \frac{2}{a_2 + a_3} \ln\left[\frac{10}{\max\{1, \frac{1}{a_5}\}}\right]. \end{aligned}$$

A.3 Sensitivity indices

The sensitivity of the fixed point to the various parameters may be studied analytically. Indeed, the equation which is satisfied by g^* is:

$$F(g, a) = n_2(g, a_{4,5}) - n_1(g, a_{1,2,3}) = 0$$

hence the partial derivatives may be directly estimated (below we assume $a_5 \geq 1$, and indeed Table A.1 suggests that $a_5 \geq 6$)

$$\frac{\partial F}{\partial g} = \frac{\partial n_2}{\partial g} - \frac{\partial n_1}{\partial g} = 0.01a_4 \frac{a_5 - 1}{(1 + 0.01g)^2} + \frac{1}{g^2} \frac{a_1}{a_2 + a_3} > 0,$$

³⁴From clinical data we observe that $a_2 + a_3 > 1$ and $a_1 = O(1)$ so that $\frac{a_1}{n(\tau)(a_2+a_3)} \ll 100$. Taking $4000 < g(0) < 8000$ and $a_2 + a_3 = 2$ we find $1.8 < \tau < 2.1$ which is similar to what is observed clinically (see Fig. 10).

$$\begin{aligned} \frac{\partial F}{\partial g} &\approx \frac{(a_4)^2(a_2 + a_3)}{a_1} + 0.01a_4(a_5 - 1), \\ \nabla_a g^* &= -\frac{\nabla_a F}{\frac{\partial F}{\partial g}} = \frac{1}{\frac{\partial n_2}{\partial g} - \frac{\partial n_1}{\partial g}} \left(\frac{\partial n_1}{\partial a_1}, \frac{\partial n_1}{\partial a_2}, \frac{\partial n_1}{\partial a_3}, -\frac{\partial n_2}{\partial a_4}, -\frac{\partial n_2}{\partial a_5} \right) \\ &= \frac{1}{\frac{\partial F}{\partial g}} \left(\frac{1}{g} \frac{1}{a_2 + a_3}, \frac{-(\frac{1}{g}a_1 + 0.1a_3)}{(a_2 + a_3)^2}, -\frac{\frac{1}{g}a_1 - 0.1a_2}{(a_2 + a_3)^2}, \right. \\ &\quad \left. -\frac{1 + 0.01 \cdot a_5 \cdot g}{1 + 0.01g}, -\frac{0.01a_4g}{1 + 0.01g} \right) \\ &= (> 0, < 0, < 0, < 0, < 0) \\ &\approx \frac{a_1}{a_4(a_2 + a_3)} \left(\frac{1}{a_1}, \frac{-1}{a_2 + a_3}, \frac{-1}{a_2 + a_3}, \frac{-1}{a_4}, \frac{-0.01a_1}{a_4(a_2 + a_3)} \right). \end{aligned}$$

We see that g^* is monotone in a_i for all i (recall that $g^* < 10\frac{a_1}{a_2}$), and that for typical parameter values (for which $g^* = O(1)$) the sensitivity to all the a_i 's except a_5 is of order one, whereas the sensitivity to a_5 is hundred folds smaller. Similarly, we can analyze the dependence of n^* on the parameters. From $n^* = n_1(g^*)$ we establish that:

$$\begin{aligned} \frac{\partial}{\partial a_{4,5}} n^* &= \frac{\partial n_1}{\partial g} \frac{\partial}{\partial a_{4,5}} g^* = \frac{-1}{\frac{\partial n_2}{\partial g} / \frac{\partial n_1}{\partial g} - 1} \frac{\partial n_2}{\partial a_{4,5}} \\ &= \frac{1}{-\frac{\partial n_2}{\partial g} / \frac{\partial n_1}{\partial g} + 1} \frac{1 + 0.01 \cdot a_5 \cdot g}{1 + 0.01g} \left(1, \frac{0.01a_4g}{1 + 0.01a_5g} \right), \end{aligned}$$

whereas $n^* = n_2(g^*)$ implies similarly that

$$\begin{aligned} \frac{\partial}{\partial a_{1,2,3}} n^* &= \frac{1}{1 - \frac{\partial n_1}{\partial g} / \frac{\partial n_2}{\partial g}} \frac{\partial n_1}{\partial a_{1,2,3}} \\ &= \frac{1}{1 - \frac{\partial n_1}{\partial g} / \frac{\partial n_2}{\partial g}} \left(\frac{1}{g} \frac{1}{a_2 + a_3}, \frac{-(\frac{1}{g}a_1 + 0.1a_3)}{(a_2 + a_3)^2}, -\frac{\frac{1}{g}a_1 - 0.1a_2}{(a_2 + a_3)^2} \right) \end{aligned}$$

hence n^* is monotone in the parameters as well. Notice that the value of r :

$$r = \left(\frac{\frac{\partial n_1}{\partial g}}{\frac{\partial n_2}{\partial g}} < 0 \right) \approx -\frac{100}{(g^*)^2} \frac{a_1}{a_4(a_2 + a_3)(a_5 - 1)} \approx -\frac{100}{a_5 - 1} \frac{a_4(a_2 + a_3)}{a_1}$$

changes the relative significance of $a_{1,2,3}$ and $a_{4,5}$ for n^* :

$$\begin{aligned} \nabla_a n^* &= \frac{\partial n_2}{\partial g} \left(\frac{\partial g^*}{\partial a_{1,2,3}}, r \frac{\partial g^*}{\partial a_{4,5}} \right) = (> 0, < 0, < 0, > 0, > 0) \\ &\approx 0.01 \left(\frac{a_5 - 1}{a_2 + a_3}, \frac{-a_1(a_5 - 1)}{(a_2 + a_3)^2}, \frac{-a_1(a_5 - 1)}{(a_2 + a_3)^2}, 100, \frac{a_1}{a_2 + a_3} \right). \end{aligned}$$

Namely, the only significant effector of n^ is a_4 .*

To complete Table 3 we use the definitions of the parameters a_i , G and N to find:

$$\begin{aligned} \frac{\partial G^*}{\partial B_G^{\max}} &= \frac{k_G}{100} \frac{\partial g^*}{\partial B_G^{\max}} = \frac{k_G}{100} \frac{\partial g^*}{\partial a_1} \frac{\partial a_1}{\partial B_G^{\max}} > 0, \\ \frac{\partial G^*}{\partial d_G^r} &= \frac{k_G}{100} \frac{\partial g^*}{\partial D_G^{r,n}} = \frac{k_G}{100} \frac{\partial g^*}{\partial a_{2,3}} \frac{\partial a_{2,3}}{\partial D_G^{r,n}} < 0, \\ \frac{\partial G^*}{\partial B_N^{\max}} &= \frac{k_G}{100} \frac{\partial g^*}{\partial a_5} \frac{\partial a_5}{\partial B_N^{\max}} < 0, \\ \frac{\partial N^*}{\partial B_N^{\max}} &= 10k_N \frac{\partial n^*}{\partial a_5} \frac{\partial a_5}{\partial B_N^{\max}} > 0, \\ \frac{\partial G^*}{\partial B_N^{\min}} &= \frac{k_G}{100} \left(\frac{\partial g^*}{\partial a_4} \frac{\partial a_4}{\partial B_N^{\min}} + \frac{\partial g^*}{\partial a_5} \frac{\partial a_5}{\partial B_N^{\min}} \right) = \frac{k_G}{100B_N^{\min}} a_4 \frac{\partial g^*}{\partial a_4} \left(1 - \frac{0.01a_5g^*}{1 + 0.01a_5g^*} \right) \\ &\approx \begin{cases} \frac{k_G}{100B_N^{\min}} a_4 \frac{\partial g^*}{\partial a_4} < 0 & \text{for } a_5g^* \ll 100, \\ \rightarrow 0 & \text{for } a_5g^* \gg 100, \end{cases} \\ \frac{\partial N^*}{\partial B_N^{\min}} &= \frac{10k_N}{B_N^{\min}} \left(a_4 \frac{\partial n^*}{\partial a_4} - a_5 \frac{\partial n^*}{\partial a_5} \right) \approx \frac{10k_N}{B_N^{\min}} a_4 \frac{\partial n^*}{\partial a_4} > 0 \quad \text{for } g^* \ll 100, \\ \frac{\partial G^*}{\partial k_G} &= \frac{g^*}{100} - \frac{a_1}{100} \frac{\partial g^*}{\partial a_1}, \\ \frac{\partial N^*}{\partial D_N} &\approx -\frac{10k_N}{D_N} \sum_{i=1}^4 a_i \frac{\partial n^*}{\partial a_i} \approx -\frac{10k_N}{D_N} a_4 \frac{\partial n^*}{\partial a_4} < 0. \end{aligned}$$

For the typical parameter values of Table A.1 $a_{iV} = (0.5, 1.38, 0.5, 1.21, 6)$ we find that $(g^*, n^*) = (0.2, 1.22)$ (similarly, for $a_{sc} = (0.5, 0.1, 3.46, 1, 9)$, $(g^*, n^*) = (0.14, 1.0)$). The partial derivatives are

$$\begin{aligned} \nabla_a g^* &\approx (0.40 \quad -0.11 \quad -0.10 \quad -0.16 \quad -0.0004), \\ \nabla_a n^* &\approx (0.024 \quad -0.0066 \quad -0.006 \quad 1.0007 \quad 0.0024550). \end{aligned}$$

Thus, we see that indeed for these typical parameters n^* is hardly sensitive to $a_{1,2,3,5}$ and is most sensitive to a_4 . For these parameters, it follows that

$$\begin{aligned} \frac{\partial G^*}{\partial B_N^{\min}} &= \frac{k_G}{100B_N^{\min}} (-0.16 + 0.0036) < 0, \\ \frac{\partial N^*}{\partial B_N^{\min}} &= \frac{10k_N}{B_N^{\min}} (1 - 0.018) > 0, \\ \frac{\partial G^*}{\partial k_G} &= \frac{g^*}{100} - \frac{a_1}{100} \frac{\partial g^*}{\partial a_1} = 0.01(0.2 - 0.2) = 0. \end{aligned}$$

To gain intuition on the dependence of the dimensional variables on the dimensional parameters, let M denote such a parameter, and let us represent it by $M = m M^{\text{typ}}$, where

M^{typ} is a fixed quantity (see Table 2). Then, we say that N^* is sensitive to changes in M if:

$$\left| \frac{N^*(M^{\text{max}}) - N^*(M^{\text{min}})}{N^*(M^{\text{typ}})} \right| \gg \left| \frac{M^{\text{max}} - M^{\text{min}}}{M^{\text{typ}}} \right|$$

so we define

$$\begin{aligned} \text{SI}(M) &= \left| \frac{N^*(M^{\text{max}}) - N^*(M^{\text{min}})}{N^*(M^{\text{typ}})} \right| \left/ \left| \frac{M^{\text{max}} - M^{\text{min}}}{M^{\text{typ}}} \right| \right. \\ &\approx \left| \frac{N^*(M^{\text{typ}})M^{\text{typ}}}{N^*(M^{\text{typ}})} \right| = \left| \frac{\left(\frac{\partial}{\partial M} N^* + \nabla_a N^* \frac{\partial a}{\partial M} \right)_{M^{\text{typ}}} M^{\text{typ}}}{N(M^{\text{typ}})} \right|. \end{aligned}$$

Since $n = \frac{N}{10k_N}$, $a_4 = \frac{1}{10} \frac{B_N^{\text{min}}}{D_N k_N}$ and $\frac{\partial n^*(a)}{\partial a_4} = 1 \gg \frac{\partial n^*(a)}{\partial a_j}$ for $j = 1, 2, 3, 5$, it follows that:

$$\text{SI}(k_N) \approx \left| n^* - \frac{B_N^{\text{min}}}{10D_N k_N} \right| = |n^* - a_4| \approx 0,$$

$$\text{SI}(B_N^{\text{min}}) \approx \text{SI}(D_N) \approx a_4$$

and all other parameters do not change much the fixed point.

References

- Abkowitz, J.L., Catlin, S.N., Guttorp, P., 1996. Evidence that hematopoiesis may be a stochastic process in vivo. *Nat. Med.* 2(2), 190–197.
- Baiocchi, G., Scambia, G., Benedetti, P., Menichella, G., Testa, U., Pierelli, L. et al., 1993. Autologous stem cell transplantation: sequential production of hematopoietic cytokines underlying granulocyte recovery. *Cancer Res.* 53(6), 1297–1303.
- Begley, C.G., Metcalf, D., Nicola, N.A., 1988. Binding characteristics and proliferative action of purified granulocyte colony-stimulating factor (G-CSF) on normal and leukemic human promyelocytes. *Exp. Hematol.* 16(1), 71–79.
- Bennett, C.L., Weeks, J.A., Somerfield, M.R. et al., 1999. Use of hematopoietic colony-stimulating factors: comparison of the 1994 and 1997 American society of clinical oncology surveys regarding ASCO clinical practice guidelines. Health services research committee of the American society of clinical oncology. *J. Clin. Oncol.* 17(11), 3676–3681.
- Bernard, S., Belair, J., Mackey, M.C., 2003. Oscillations in cyclical neutropenia: new evidence based on mathematical modeling. *J. Theor. Biol.* 222(3), 283–298.
- Blumenson, L.E., Bross, I.D., 1979. Assessment of myelotoxic effects of chemotherapy from early leukopenic response: application of a mathematical model for granulopoiesis. *J. Surg. Oncol.* 11(2), 171–176.
- Bodensteiner, D.C., Doolittle, G.C., 1993. Adverse haematological complications of anticancer drugs. Clinical presentation, management and avoidance. *Drug Saf.* 8(3), 213–224.
- Bonig, H.B., Hannen, M., Lex, C., Wolfel, S., Banning, U., Nurnberger, W. et al., 1999. Additive effects of infection and neutropenia on the induction of granulocytopoietic activity in vivo. *Cancer* 86(2), 340–348.
- Bonilla, M.A., Gillio, A.P., Ruggeiro, M., Kernan, N.A., Brochstein, J.A., Abboud, M. et al., 1989. Effects of recombinant human granulocyte colony-stimulating factor on neutropenia in patients with congenital agranulocytosis. *NEJM* 320, 1574–1580.
- Bronchud, M.H., Potter, M.R., Morgenstern, G. et al., 1988. In vitro and in vivo analysis of the effects of recombinant human granulocyte colony-stimulating factor in patients. *Br. J. Cancer* 58, 64–69.

- Carulli, G., Marini, A., Azzara, A., Vanacore, R., Petrini, M., 2000. Cyclic oscillations of neutrophils, monocytes, and cd8-positive lymphocytes in a healthy subject. *Haematologica* 85(4), 447–448.
- Clark, O.A., Lyman, G.H., Castro, A.A., Clark, L.G., Djulbegovic, B., 2005. Colony-stimulating factors for chemotherapy-induced febrile neutropenia: a meta-analysis of randomized controlled trials. *J. Clin. Oncol.* 23, 4198–4214.
- Colotta, F., Re, F., Polentarutti, N., Sozzani, S., Mantovani, A., 1992. Modulation of granulocyte survival and programmed cell death by cytokines and bacterial products. *Blood* 80(8), 2012–2020.
- Crawford, J., Dale, D.C., Lyman, G.H., 2004. Chemotherapy-induced neutropenia: risks, consequences, and new directions for its management. *Cancer* 100, 228–237.
- Cronkite, E.P., 1979. Kinetics of granulocytopoiesis. *Clin. Haematol.* 8, 351–370.
- Dancey, J.T., Deubelbeiss, K.A., Harker, L.A., Finch, C.A., 1976. Neutrophil kinetics in man. *J. Clin. Invest.* 58(3), 705–715.
- de Haas, M., Kerst, J.M., Van der Schoot, C.E., Calafat, J., Hack, C.E., Nuijens, J.H. et al., 1994. Granulocyte colony-stimulating factor administration to healthy volunteers: analysis of the immediate activating effects on circulating neutrophils. *Blood* 84(11), 3885–3894.
- Donnelly, G.B., Glassman, J., Long, C. et al., 2000. Granulocyte-colony stimulating factor (G-CSF) may improve disease outcome in elderly patients with diffuse large cell lymphoma (DLCL) treated with CHOp chemotherapy. *Leuk. Lymphoma* 39(1–2), 67–75.
- Fliedner, T.M., Graessle, D., Paulsen, C., Reimers, K., 2002. Structure and function of bone marrow hemopoiesis: mechanisms of response to ionizing radiation exposure. *Cancer Biother. Radiopharm.* 17(4), 405–426.
- Foley, C., Bernard, S., Mackey, M.C., 2006. Cost-effective G-CSF therapy strategies for cyclical neutropenia: mathematical modelling based hypotheses. *J. Theor. Biol.* 238, 637–754.
- Freedman, D.A., 2004. Graphical models for causation, and the identification problem. *Eval. Rev.* 28, 267–293.
- Friberg, L.E., Karlsson, M.O., 2003. Mechanistic models for myelosuppression. *Invest. New Drugs* 21(2), 183–194.
- Fukuda, M., Oka, M., Ishida, Y., Kinoshita, H., Terashi, K., Fukuda, M. et al., 2001. Effects of renal function on pharmacokinetics of recombinant human granulocyte colony-stimulating factor in lung cancer patients. *Antimicrob. Agents Chemother.* 45(7), 1947–1951.
- Gisslinger, H., Kurzrock, R., Wetzler, M., Tucker, S., Kantarjian, H., Robertson, B., Talpaz, M., 1997. Apoptosis in chronic myelogenous leukemia: studies of stage-specific differences. *Leuk. Lymphoma* 25, 121–133.
- Guckenheimer, J., Holmes, P., 2002. *Nonlinear Oscillations, Dynamical Systems, and Bifurcations of Vector Fields*. Springer, Berlin.
- Haurie, C., Dale, D.C., Rudnicki, R., Mackey, M.C., 2000. Modeling complex neutrophil dynamics in the grey collie. *J. Theor. Biol.* 204, 505–519.
- Hollenstein, U., Homoncik, M., Stohlawetz, P.J., Marsik, C., Sieder, A., Eichler, H.G., Jilma, B., 2000. Endotoxin down-modulates granulocyte colony-stimulating factor receptor (cd114) on human neutrophils. *J. Infect. Dis.* 182(1), 343–346.
- Joyce, R.A., Boggs, D.R., Chervenick, P.A., 1976. Neutrophil kinetics in hereditary and congenital neutropenias. *N. Engl. J. Med.* 295(25), 1385–1390.
- Kawakami, M., Tsutsumi, H., Kumakawa, T., Abe, H., Hirai, M., Kurosawa, S. et al., 1990. Levels of serum granulocyte colony-stimulating factor in patients with infections. *Blood* 76, 1962–1964.
- Kenneth, V.I., Rolston, M.D., Gerald, P., Bodey, M.D., 2000. *Infections in Patients with Cancer*, 5th edn. Decker, Hamilton.
- Kimura, A., Sultana, T.A., 2004. Granulocyte colony-stimulating factor receptors on CD34++ cells in patients with myelodysplastic syndrome (MDS) and MDS-acute myeloid leukemia. *Leuk. Lymphoma* 45, 1995–2000.
- King-Smith, E.A., Morley, A., 1970. Computer simulation of granulopoiesis: normal and impaired granulopoiesis. *Blood* 36, 254–262.
- Kotto-Kome, A.C., Fox, S.E., Lu, W., Yang, B.B., Christensen, R.D., Calhoun, D.A., 2004. Evidence that the granulocyte colony-stimulating factor (g-csf) receptor plays a role in the pharmacokinetics of g-csf and pegg-csf using a g-csf-r ko model. *Pharmacol. Res.* 50(1), 55–58.
- Krishan, A., Pitman, S.W., Tattersall, H.N., Paika, K.D., Smith, D.C., Frei, E., III, 1976. Flow microfluorometric patterns of human bone marrow and tumor cells in response to cancer chemotherapy. *Cancer Res.* 36(10), 3813–3820.

- Krishnan, S., Chi, E.Y., Webb, J.N., Chang, B.S., Shan, D., Goldenberg, M. et al., 2002. Aggregation of granulocyte colony stimulating factor under physiological conditions: characterization and thermodynamic inhibition. *Biochemistry* 41(20), 6422–6431.
- Krishnaswamy, G., Kelley, J., Yerra, L., Smith, J.K., Chi, D.S., 1999. Human endothelium as a source of multifunctional cytokines: molecular regulation and possible role in human disease. *J. Interf. Cytokine Res.* 19(2), 91–104.
- Kroger, N., Sonnenberg, S., Cortes-Dericks, L., Freiberger, P., Mollnau, H., Zander, A.R., 2004. Kinetics of G-CSF and CD34+ cell mobilization after once or twice daily stimulation with rHu granulocyte-stimulating factor (lenograstim) in healthy volunteers: an intraindividual crossover study. *Transfusion* 44(1), 104–110.
- Krzyzanski, W., Ramakrishnan, R., Jusko, W.J., 1999. Basic pharmacodynamic models for agents that alter production of natural cells. *Pharmacokinet. Biopharm.* 27, 467–489.
- Ladd, A.C., Pyatt, R., Gothot, A., Rice, S., McMahon, J., Christie, M. et al., 1997. Orderly process of sequential cytokine stimulation is required for activation and maximal proliferation of primitive human bone marrow CD34+ hematopoietic progenitor cells residing in g0. *Blood* 90, 658–668.
- Lajtha, L.G., Oliver, R., Gurney, C.W., 1962. Kinetic model of a bone-marrow stem-cell population. *Brit. J. Haemat.* 8, 442–460.
- Lieschke, G.J., Grail, D., Hodgson, G., Metcalf, D., Stanley, E., Cheers, E. et al., 1994. Mice lacking granulocyte colony-stimulating factor have chronic neutropenia, granulocyte and macrophage progenitor cell deficiency, and impaired neutrophil mobilization. *Blood* 84, 1737–1746.
- Lord, B.I., Bronchud, M.H., Owens, S., Chang, J., Howell, A., Souza, L. et al., 1989. The kinetics of human granulopoiesis following treatment with granulocyte colony stimulating factor in vivo. *Proc. Natl. Acad. Sci. USA* 86, 9499–9503.
- Marley, S.B., Gordon, M.Y., 2005. Chronic myeloid leukaemia: stem cell derived but progenitor cell driven. *Clin. Sci. (Lond.)* 109, 13–25.
- Molineux, G., 2003. Pegfilgrastim: using pegylation technology to improve neutropenia support in cancer patients. *Anticancer Drugs* 14, 259–264.
- Moore, M.A., 1991. Clinical implications of positive and negative hematopoietic stem cell regulators. Review: Stratton lecture 1990. *Blood* 78, 1–19.
- Mukae, H., Zamfir, D., English, D., Hogg, J.C., van Eeden, S.F., 2000. Polymorphonuclear leukocytes released from the bone marrow by granulocyte colony-stimulating factor: intravascular behavior. *Hematol. J.* 1(3), 159–171.
- Noursadeghi, M., Pepys, M.B., Gallimore, R., Cohen, J., 2005. Relationship of granulocyte colony stimulating factor with other acute phase reactants in man. *Clin. Exp. Immunol.* 140(1), 97–100.
- Ostby, I., Rusten, L.S., Kvalheim, G., Grottum, P., 2003. A mathematical model for reconstitution of granulopoiesis after high dose chemotherapy with autologous stem cell transplantation. *J. Math. Biol.* 47(2), 101–136.
- Panetta, J.C., Kirstein, M.N., Gajjar, A.J., Nair, G., Fouladi, M., Stewart, C.F., 2003. A mechanistic mathematical model of temozolomide myelosuppression in children with high-grade gliomas. *Math. Biosci.* 186(1), 29–41.
- Pigoli, G., Waheed, A., Shaddock, R.K., 1982. Observations on the binding and interaction of radiolabeled colony-stimulating factor with murine bone marrow cells in vivo. *Blood* 59(2), 408–420.
- Pollmacher, T., Korth, C., Schreiber, W., Hermann, D., Mullington, J., 1996. Effects of repeated administration of granulocyte colony-stimulating factor (G-CSF) on neutrophil counts, plasma cytokine, and cytokine receptor levels. *Cytokine* 8, 799–803.
- Price, T.H., Chatta, G.S., Dale, D.C., 1996. Effect of recombinant granulocyte colony-stimulating factor on neutrophil kinetics in normal young and elderly humans. *Blood* 88, 335–340.
- Price, T.H., Raleigh, A., Bowden, R.A., Boeckh, M., Bux, J., Nelson, K. et al., 2000. Phase I/II trial of neutrophil transfusions from donors stimulated with G-CSF and dexamethasone for treatment of patients with infections in hematopoietic stem cell transplantation. *Blood* 95, 3302–3309.
- Ratajczak, M.Z., Gewirtz, A.M., 1995. The biology of hematopoietic stem cells. *Semin. Oncol.* 22, 210–217.
- Rubinow, S.I., Lebowitz, J.Z., 1975. A mathematical model of neutrophil production and control in normal man. *J. Math. Biol.* 1, 187.
- Sachs, L., 1992. The molecular control of haematopoiesis: from cell cultures to the clinic. In: *Molograstim GM-CSF: Possibilities and Perspectives*, p. 311. Royal Society of Medicine Services, London.
- Saito, S., Kawano, Y., Watanabe, T., Okamoto, Y., Abe, T., Kurada, Y., Takaue, Y., 1999. Serum granulocyte colony-stimulating factor kinetics in children receiving intense chemotherapy with or without stem cell support. *J. Hematother.* 8, 291–297.

- Sallerfors, B., 1994. Endogenous production and peripheral blood levels of granulocyte-macrophage (GM-) and granulocyte (G-) colony-stimulating factors. *Leuk. Lymphoma* 13(3-4), 235–247.
- Sarkar, C.A., Lauffenburger, D.A., 2003. Cell-level pharmacokinetic model of granulocyte colony-stimulating factor: implications for ligand lifetime and potency in vivo. *Mol. Pharmacol.* 63(1), 147–158.
- Scholz, M., Engel, C., Loeffler, M., 2005. Modelling human granulopoiesis under poly-chemotherapy with G-CSF support. *J. Math. Biol.* 50(4), 397–439.
- Selig, C., Nothdurft, W., 1995. Cytokines and progenitor cells of granulocytopenia in peripheral blood of patients with bacterial infections. *Infect. Immun.* 63(1), 104–109.
- Shochat, E., Stemmer, S.M., Segel, L., 2002. Human haematopoiesis in steady state and following intense perturbations. *Bull. Math. Biol.* 64(5), 861–886.
- Smaaland, R., Laerum, O.D., Sothorn, R.B., Sletvold, O., Bjerknes, R., Lote, K., 1992. Colony-forming unit-granulocyte-macrophage and DNA synthesis of human bone marrow are circadian stage-dependent and show covariation. *Blood* 79(9), 2281–2287.
- Stute, N., Santana, V.M., Rodman, J.H., Schell, M.J., Ihle, J.N., Evans, W.E., 1992. Pharmacokinetics of subcutaneous recombinant human granulocyte colony-stimulating factor in children. *Blood* 79, 2849–2854.
- Takatani, H., Soda, H., Fukuda, M., Watanabe, M., Kinoshita, A., Nakamura, T., Oka, M., 1996. Levels of recombinant human granulocyte colony-stimulating factor in serum are inversely correlated with circulating neutrophil counts. *Antimicrob. Agents Chemother.* 40(4), 988–991.
- Taveira da Silva, A.M., Kaulbach, H.C., Chuidian, F.S., Lambert, D.R., Suffredini, A.F., Danner, R.L., 1993. Brief report: shock and multiple-organ dysfunction after self-administration of salmonella endotoxin. *N. Engl. J. Med.* 328(20), 1457–1460.
- Terashi, K., Oka, M., Ohdo, S., Furukubo, T., Ikeda, C., Fukuda, M. et al., 1999. Close association between clearance of recombinant human granulocyte colony-stimulating factor (G-CSF) and G-CSF receptor on neutrophils in cancer patients. *Antimicrob. Agents Chemother.* 43(1), 21–24.
- Thiele, J., Kvasnicka, H.M., 2002. CD34+ stem cells in chronic myeloproliferative disorders. *Histol. Histopathol.* 17, 507–521.
- Vainstein, V., Ginosar, Y., Shoham, M., Ranmar, D.O., Ianovski, A., Agur, Z., 2005. The complex effect of granulocyte colony-stimulating factor on human granulopoiesis analyzed by a new physiologically-based mathematical model. *J. Theor. Biol.* 234(3), 311–327.
- Van der Auwera, P., Platzer, E., Xu, Z.X., Schulz, R., Feugeas, O., Capdeville, R., Edwards, D.J., 2001. Pharmacodynamics and pharmacokinetics of single doses of subcutaneous pegylated human G-CSF mutant (Ro 25-8315) in healthy volunteers: comparison with single and multiple daily doses of filgrastim. *Am. J. Hematol.* 66(4), 245–251.
- Wang, B., Ludden, T.M., Cheung, E.N., Schwab, G.G., Roskos, L.K., 2001. Population pharmacokinetic-pharmacodynamic modeling of filgrastim (r-methug-csf) in healthy volunteers. *J. Pharmacokinet. Pharmacodyn.* 28(4), 321–342.
- Weiss, M., Voglic, S., Harms-Schirra, B., Lorenz, I., Lasch, B., Dumon, K. et al., 2003. Effects of exogenous recombinant human granulocyte colony-stimulating factor (filgrastim, rhg-csf) on neutrophils of critically ill patients with systemic inflammatory response syndrome depend on endogenous G-CSF plasma concentrations on admission. *Intensive Care Med.* 29(6), 904–914.
- Wen, W., Guanlin, S., Guoxiong, T., Zhenyi, W., 2001. Serum granulocyte colony-stimulating factor in patients with chronic renal failure. *Chin. Med. J.* 114, 596–599.
- Zamboni, W.C., D'Argenio, D.Z., Stewart, C.F., MacVittie, T., Delauter, B.J., Farese, A.M. et al., 2001. Pharmacodynamic model of topotecan-induced time course of neutropenia. *Clin. Cancer Res.* 7(8), 2301–2308.
- Zarkovic, M., Kwaan, H.C., 2003. Correction of hyperviscosity by apheresis. *Semin. Thromb. Hemost.* 29(5), 535–542.